AD NUMBER

ADB157706

NEW LIMITATION CHANGE

TO

Approved for public release, distribution unlimited

FROM

Distribution authorized to U.S. Gov't. agencies only; Proprietary Info.; 1 Jun 91. Other requests shall be referred to HQS, CAC & Ft. Leavenworth, Attn: ATZL-GOP-SE. Ft. Leavenworth, KS 66027-6900.

AUTHORITY

USACGSC ltr, 2 May 2001.

FINITE ELEMENT ANALYSIS OF LASER-INDUCED DAMAGE TO MECHANICALLY LOADED LAMINATED COMPOSITES IN HELICOPTERS

A thesis presented to the Faculty of the U.S. Army Command and General Staff College in partial fulfillment of the requirements for the degree

MASTER OF MILITARY ART AND SCIENCE

by
MOHAMMED J.K. ALGHATAM, LTC, BDF, BAHRAIN
Ph.D., M.Sc., B.Sc., C.Eng., M I Mech. Eng.,
Mem. ASME., Mem. IACM.

Fort Leavenworth, Kansas
1991

REPORT DOCUMENTATION PAGE

Form Approved
OMB No. 0704-0188

1. AGENCY USE ONLY (Leave blank)	2. REPORT DATE	3. REPORT TYPE AND DATES COVERED
	7th, June, 1991	Master's Thesis 1 Aug 90 - 7 Jun 91

4. TITLE AND SUBTITLE Finite Element Analysis of Laser-Induced Damage to Mechanically Loaded Laminated Composites in Helicopters.

5. FUNDING NUMBERS

6. AUTHOR(S)

LTC MOHAMMED J.K. ALGHATAM

7. PERFORMING ORGANIZATION NAME(S) AND ADDRESS(ES)

Command and General Staff College
Attn: ATZL-SWD-GD
Fort Leavenworth, KS 66027-6900

8. PERFORMING ORGANIZATION REPORT NUMBER

9. SPONSORING/MONITORING AGENCY NAME(S) AND ADDRESS(ES)

10. SPONSORING/MONITORING AGENCY REPORT NUMBER

11. SUPPLEMENTARY NOTES

12a. DISTRIBUTION/AVAILABILITY STATEMENT Distribution authorized to U.S. agencies only; proprietary information, 1 June 1991. Other requests for this document must be referred to: HQs, CAC & Ft. Leavenworth, ATTN: ATZL-GOP-SE, Ft. Leavenworth, KS 66027 5070.

12b. DISTRIBUTION CODE

13. ABSTRACT *(Maximum 200 words)*

This thesis examines the lethality of laser-directed energy weapons in causing structural failure to mechanically loaded laminated composites in helicopters. The analysis is based on a three-dimensional numerical finite element model of a rectangular, incipient, orthotropic compression panel with its edges rotationally restrained. The panel is made of 24"x6" graphite/epoxy laminated composite where the laminate consists of fourteen laminas of different ply orientation angles and two different thicknesses. Laser irradiation beam strikes the center lines of the panel with a radius of 3" and applied power load of 1KW/sq cm causing an intense localized heating to the already mechanically loaded panel. Mechanical and thermal buckling and post-buckling behavior of the heated panel are predicted, which is complicated by the anisotropic behavior of the composite material and the thermal effect. Even without buckling, the problem is thermally and structurally non-linear. This work provides insight into using existing codes to obtain approximate solutions good enough for the engineering design, with speed and low cost. This knowledge to the designer of directed energy laser weapon can optimize designs of future weapons, or efficient use of existing ones. Likewise, the helicopter structural designer can optimize the design of future panels and structures, or the efficient use of existing ones.

14. SUBJECT TERMS	15. NUMBER OF PAGES
FINITE ELEMENT, LASER, COMPOSITES, LAMINATED, HEAT TRANSFER, BUCKLING, TEMPERATURE, ENERGY WEAPONS, ANALYSIS, 3-D, INCIPIENT, ORTHOTROPIC, COMPRESSION, ANISOTROPIC, GRAPHITE, EPOXY, HELICOPTERS	120
	16. PRICE CODE

17. SECURITY CLASSIFICATION OF REPORT	18. SECURITY CLASSIFICATION OF THIS PAGE	19. SECURITY CLASSIFICATION OF ABSTRACT	20. LIMITATION OF ABSTRACT
UNCLASSIFIED	UNCLASSIFIED	UNCLASSIFIED	UL

MASTER OF MILITARY ART AND SCIENCE
THESIS APPROVAL PAGE

Name of candidate: LTC Mohammed J.K. Alghatam

Title of thesis: Finite Element Analysis of Laser-Induced Damage to Mechanical'y Loaded Laminated Composites in Helicopters.

Approved by:

_____, Thesis Committee Chairman
Mr. James F. Fox, M.A., B.A.

_____, Member
Mr. David I. Drummond, M.S., B.S.

_____, Member
CPT George J. Fukumoto, B.S.

Accepted this 7th day of June 1991 by:

_____, Director, Graduate Degree Programs
Philip J. Brookes, Ph.D.

The opinions and conclusions expressed herein are those of the student author and do not necessarily represent the views of the U.S. Army Command and General Staff College or any other governmental agency. (References to this study should include the foregoing statement.

ABSTRACT

FINITE ELEMENT ANALYSIS OF LASER-INDUCED DAMAGE TO MECHANICALLY LOADED LAMINATED COMPOSITES IN HELICOPTERS, by LTC Mohammed J.K. Alghatam, BDF, Bahrain, 113 pages.

This thesis examines the lethality of laser-directed energy weapons in causing structural failure to mechanically loaded laminated composites in helicopters. The analysis is based on a three-dimensional numerical finite element model of a rectangular, incipient, orthotropic compression panel with its edges rotationally restrained. The panel is made of 24"x6" graphite/epoxy laminated composite where the laminate consists of fourteen laminas of different ply orientation angles and two different thicknesses.

The data for the degradation of the material properties with increasing temperature, as well as temperature dependence thermal response data, were provided by the Naval Research Laboratory, Washington, D.C. Laser irradiation beam strikes the center lines of the panel with a radius of 3" and applied power load of 1 kilowatt per square centimeter causing an intense localized heating to the already mechanically loaded panel.

Failure of laminated composites is controversial, even under ambient temperature. However, a successful attempt has been conducted here to predict the mechanical and thermal buckling and post-buckling behavior of the heated panel. This is further complicated by the anisotropic behavior of the composite material and the thermal effect. Even without buckling, the problem is thermally and structurally non-linear. This work can be considered as an above preliminary numerical analysis. It provides insight (to be verified by experimentation) into using existing codes to obtain approximate solutions good enough for the engineering design, with speed and low cost.

Should this expertise and knowledge be available, the designer of directed energy laser weapon can optimize designs of future weapons, or make efficient use of existing ones. Likewise, the helicopter structural designer can optimize the design of future panels and structures, or make efficient use of existing ones. In addition, the designer can tailor a composite material to meet a particular structural requirement with little waste of material capability. The ability to tailor a composite material to its job is the biggest advantage that composites have over metallic or plastic structures. The complete prediction gives the values of static and thermal loads, stresses, strains, and various other heat transfer parameters throughout the domain of interest.

Finite element method superiority to other numerical analysis techniques is evident and numerical results of this work compare favorably with experimental results.

ACKNOWLEDGMENTS

Sincerest thanks are owed to Dr. Philip J. Brookes, Director, Graduate Degree Programs, for allowing me this participation in order to acquire the degree of Master of Military Art and Science.

I would like to take this opportunity to express my thanks to my research committee chairman, Mr. James F. Fox, for the early useful discussions, interest, encouragement, and for making this thesis subject idea available in conjunction with the Naval Research Laboratory (NRL), Washington, D.C.

My profound gratitude goes to the second reader and member of my research committee, Mr. David I. Drummond, for his continuous help, deep interest and guidance, for whom this work would not have been possible without his active assistance throughout.

Kind appreciation is due to CPT George J. Fukumoto, the consulting faculty member in my research committee for the part he played under the direction of the chairman with regard to the arrangements with the NRL in Washington, D.C.

Special thanks and appreciation are due to Dr. Ronald C. Gularte, Head, Engineering Materials Group, NRL, Washington, D.C., for the useful discussions, interest, effective help and guidance at certain stages of this work.

Thanks are also attributed to both Dr. Victor Weingarten, and Dr. Lashkari of the Structural Research and Analysis Corporation (SRAC), Santa Monica, California, for allowing me to run this thesis finite element model on their corporation's well known finite element, personal computer package (COSMOS/M).

Finally, I wish to thank the Bahrain Defense Force (BDF) for the financial support provided while I was doing my Command and General Staff Officer Course (CGSOC) at Fort Leavenworth, which gave me the opportunity to pursue this thesis.

TABLE OF CONTENTS

LIST OF FIGURES

LIST OF FIGURES (Continued)

CHAPTER 1

INTRODUCTION

This work concerns the current directed energy program investigating lethality of lasers and its support. A laser load of sufficient magnitude can cause structural failure for ballistic missiles, fixed-wing planes, and helicopters. Laser loading can damage main structural components or vulnerable internal components, which can result in the failure of the missile or aircraft mission.

Therefore, it is necessary to understand the response of laminated composite thin shell structure to sudden and intense loading. The objective of the approach is to develop a three-dimensional numerical finite element model and predict the response of mechanically loaded and intensely localized spot heated composite structures in helicopters. The reason for using numerical methods is due to the anticipated and already practically verified non-linearity of the thermal and mechanical responses.

It should be emphasized that the subject of the failure of laminated composites is controversial, even under ambient temperatures. Since the processes under consideration have a very important impact in directed energy weapon environment, they should be dealt with effectively. This can be done as a result of understanding the processes and their nature and the ability to predict them quantitatively. If this expertise and knowledge is available, the designer of a directed energy laser weapon can ensure the desired performance and can choose an optimum design from many alternate possibilities. Also the power of prediction enables the operation of existing laser weapons more efficiently. On the other hand, the helicopter structural designer can determine critical laminated composite panels of the structure needing strengthening or redundancy to survive laser strikes at a relatively low cost.

The prediction of behavior in a given physical situation requires the values of the relevant variables governing the process of interest.[1] In this thesis work on directed energy laser weapons against helicopters, the complete prediction gives us the values of static and thermal loads, stresses, and strains; it also provides heat transfer parameters such as temperature distributions throughout the domain of interest.

Actual measurement gives the most reliable information about any physical process. Since the Naval Research Laboratory (NRL) has conducted

[1]S. V. Patankar, Numerical Heat Transfer and Fluid Flow (New York: Hemisphere Publishing Corporation, McGraw-Hill Book Company, 1980), p. 12.

such experiments, they were kind enough to forward all available physical data.

As for the numerical method we are going to use the theoretical prediction, it works out the results of a mathematical model consisting of a set of non-symmetrical, and non-linear partial differential equations. The theoretical calculations offer many advantages over a corresponding experimental investigation. Such advantages are apparent in low cost, speed, complete information, and ability to simulate realistic and ideal conditions. Still, there are drawbacks and limitations, the most important of which is that the validity of the mathematical model limits the usefulness of the computation.

This work involves a difficult problem of complex composites geometry and sensitive materials properties, as well as non-linearities. The extremely intense high temperatures, incipient structures with post-buckled loadings and spot heating, make it hard to solve numerically. Up to now, to the best of the author's knowledge, no one has analyzed the problem of laser damage in loaded laminated composite panels (as configured here) using the finite element method.

The finite element method is a general numerical method based on an approximate solution of a continuum problem that allows an immediate extension to non-structural problems. We define continuum as a body of matter (solid, liquid, gas, or plasma) or simply a region of space in which a

particular phenomenon is occurring.[2] Quantities with obvious physical meaning are chosen as the variable parameters, hence giving a direct physical contact with the real problem being examined.

The label "finite element method" first appeared in 1954, when it was used by R.W. Clough[3] in a paper on plane elasticity problems, but the ideas of finite element analysis date back much further.

The foundation of framework analysis was laid in the period 1850-1875 by Maxwell and Mohr, amongst others. These concepts provide the methodology of matrix structural analysis that underlies finite element theory. A lack of quick solution methods for multiple algebraic equations prevented any true further advance for eighty years. These limitations were relieved somewhat in 1932 when Hardy Cross introduced the method of Moment Distribution. This made it feasible to solve more complex problems by orders of magnitude.

The introduction of the computer in the 1950s gave a means of handling quickly the previously unsolvable matrix algebra. The solution of real problems dealing with complex continua by limiting their infinite degrees of freedom to a finite number of unknowns became possible. Such a process

---

[2]Mohammed J. Alghatam "An Investigation into the Use of the Finite Element Method for Certain Continuum Problems" (Unpublished MSC thesis, University of Technology, Loughborough, Leics, England, UK, 1979), p. 1.

[3]Robert W. Clough, "The Finite Element Method in Structural Mechanics," in Stress Analysis: Recent Developments in Numerical and Experimental Methods, ed. by O.C. Zienkiewicz and G.S. Holister (London: Wiley and Sons Ltd., 1954), pp. 48-79.

of discretization was first successfully performed by the now well known method of "Finite Differences."

The mid-fifties saw the arrival of another approach, that of finite elements. Its somewhat simple logic makes it ideally suited for the computer. The first elements evolved were by Turner, Clough,[4] and Melosh, triangular, rectangular, and plate bending respectively.

Although originally derived to study stress in complex airframe structural problems, finite element methods have expanded into such fields as heat transfer and fluid flow. This extension process of the finite element technique (the variational approach) to non-structural situations, was documented by O.C. Zienkiewicz and Cheung in 1965.[5,6,7]

The finite element method, as a numerical analysis technique for obtaining approximate solutions to a wide variety of engineering problems, has extended and been applied to the broad field of continuum mechanics. The finite element method has received much attention in engineering schools and industry due to its diversity and flexibility as an analytical tool.

---

[4]Ibid, pp. 48-79.

[5]O. C. Zienkiewicz, The Finite Element Method (London: McGraw-Hill Book Company, 1977), p. 435.

[6]Y. K. Cheung and M. F. Yeo, Practical Introduction to Finite Element Analysis (London: Pitman Publishing Co., 1979), p. 112.

[7]O. C. Zienkiewicz, "The Finite Element Method: From Intuition to Generality." Applied Mechanics Review (London: McGraw-Hill Book Company, 1969), p. 19.

In continuum problems of any dimensions, the field variables (whether pressure, temperature, displacement, stress, or any other quantity) possess an infinite number of values because it is a function of each generic point in the body or solution region. Therefore, the problem has an infinite number of unknowns. The finite element discretization procedure reduces the problem to one of a finite number of unknowns by dividing the solution region into elements and by expressing the unknown field variable in terms of assumed approximate functions within each element.

The approximate functions, also called interpolation functions or shape functions, are defined in terms of the field variable values at specified points called nodes that usually lie on element boundaries where adjacent elements are considered to be connected.[8] In addition to boundary nodes, an element also may have few interior nodes. The behavior of the field variables within the elements is completely defined by the nodal values of the field variables and shape functions. For the finite element representation of a problem, the nodal values of the field variable become the new unknowns. Once these unknowns are found, the shape functions define the field variables through the assemblage elements.[9]

---

[8]K. H. Huebner, The Finite Element Method for Engineers (London: Wiley and Sons Ltd., 1975), p. 38.

[9]Alghatam, "An Investigation into the Use of the Finite Element Method for Certain Continuum Problems," pp. 25-32.

The nature of the solution and the degree of the approximation depend not only on the size and number of the elements used, but also on the shape functions selected. Functions cannot be chosen arbitrarily because certain compatibility conditions should be satisfied. Often functions are chosen so that the field variable or its derivatives are continuous across adjoining element boundaries.

An important feature of the finite element method, which sets it apart from other approximate methods, is the ability to formulate solutions for individual elements before putting them together to represent the entire problem. This means that complex problems can be reduced by considering a series of greatly simplified problems.

Another advantage of the finite element method is the variety of ways in which one can formulate the properties of individual elements and even change them within the solution iterations. This applies to the fluid or continuum properties too.

The major advantages of the finite element method over the better established finite difference method lies in the ease that problems involving complicated irregular geometries and arbitrary local mesh refinement can be incorporated.

The present finite element solution of the three-dimensional Cartesian coordinate laser-induced damage to mechanically loaded laminated

composite panel of a helicopter is compared with experimental results obtained from the NRL, Washington, D.C.

It was desirable in this thesis to have the finite element numerical method of solution predict the physical behavior and the stress patterns and associated heat transfer processes. Great emphasis during the present investigation has been placed on the development of both computational and modeling techniques that contribute to the efficiency of the finite element method as applied to real-time coupled stress and heat transfer. A major objective of this work is to show the applicability and flexibility of the finite element method in solving continuum, real-time problems. A good insight into the theory and applications of the finite element method can be found in scientific writings[10,11,12,13] of diverse fields of engineering such as: vibration, stress analysis, heat transfer, fluid flow, and solar energy. In order to get a reasonable grasp of the foundation knowledge and fundamentals of the

---

[10]Mohammed J. Alghatam, "The Forced Vibration of Beams and Frameworks Using the Finite Element Method" (unpublished BSC Thesis, Trent Polytechnic, Nottingham, England, UK, 1976), pp. 1-108.

[11]Alghatam, "An Investigation into the Use of the Finite Element Method for Certain Continuum Problems," pp. 1-178.

[12]Mohammed J. Alghatam, "Solar Ventilation and Air-Conditioning System Investigation Using the Finite Element Method" (Unpublished PhD Thesis, University of Technology, Loughborough, Leics, England, UK, 1985), pp. 1-722.

[13]Mohammed J. K. Alghatam, "Solar-Powered Air Conditioning System Investigation Using Finite Element Method," Solar And Wind Technology, Vol. 4, No. 3 (Oxford: Pergamon Press, 1987), pp. 243-268.

numerical analysis and the finite element method and techniques, several specific references[14,15,16,17] provide an outstanding source.

The four basic approaches for formulating the finite element to obtain element properties,[18] are as follows:

1. The direct approach (traceable in origin to stiffness method of structural analysis);
2. The variational approach (more versatile and advanced);
3. The weighted residual approach (even more versatile and advanced, but might be less respectable mathematically;
4. The energy balance approach (relies on the balance of thermal and/or mechanical energy of a system).

Regardless of the approach used to find the element properties, the solution of a continuum problem by the finite element method is always in the following six steps:[19]

---

[14]S. Scheid, "Numerical Analysis," Schaum's Outline Series (New York: McGraw-Hill, 1968) pp. 40-72.

[15]J. Timothy Oden, Finite Elements of Non-linear Continua (New York: McGraw-Hill, 1972), pp. 1-131.

[16]L. J. Segerlind, Applied Finite Element Analysis (London: Wiley and Sons Ltd., 1976), pp. 12-98.

[17]E. Hinton and D. R. Owen, Finite Element Programming (Swansea: Academic Press, 1977), pp. 1-120.

[18]Alghatam, "An Investigation into the Use of the Finite Element Method for Certain Continuum Problems," pp. 2-4.

[19]Ibid, pp. 2-4.

1. Discretization of the continuum: dividing the domain into elements;
2. Selection of interpolation functions: shape functions;
3. Finding the element properties: matrix equations expressing element properties are found using one of the four approaches just mentioned;
4. Assembling element properties to obtain the system equations: combining matrix equations of the elements' behavior to form overall matrix equations expressing the behavior of the entire solution region, domain, or system. The matrix equations for the system have the same form as the equations for an individual element except that they contain many more terms because they include all nodes. Also at this stage the boundary conditions are introduced into the global assembly matrix. The basis of the assembly is that at shared node between two or more elements, value of the field variable is the same for each element sharing the node;[20]
5. Solution of the system equations: solving the set of linear or non-linear simultaneous partial differential equations;
6. Making additional computations if desired: sometimes the solution of the system equations is used to calculate other

[20]Huebner, "The Finite Element Method for Engineers," pp. 49-56.

important parameters, e.g., calculating heat flux from known temperature field.

In this work the discretization process of the stress part is done via the strain energy method while that of the thermal part is carried out by means of the error distribution principle (Galerkin method), using weighted residuals, where the weighting functions used need not be the same as the interpolation (shape) functions for the element (Petrov-Galerkin). In each case integration by parts (Green's theorem) is used to invoke the boundary conditions. The governing non-linear partial differential equations are transformed into "finite element equations" governing all isolated elements. These local elements are finally collected together to form a global system of non-linear partial differential equations or "algebraic equations" with proper boundary and/or initial conditions imposed. The use of suitable boundary conditions makes the coefficient matrix non-singular and not ill-conditioned, thus allowing a solution to be obtained. The type of element used is the eight noded isoparametric quadrilateral three-dimensional (brick) element (Serendipity family). Within the next few months a specially formulated laminated composite finite element will be available in the Finite Element/Personal Computer (F.E./P.C.) package, COSMOS/M of the Structural Research and Analysis Corporation (SRAC), used in this thesis.

This thesis consists of seven chapters. The first chapter introduces the subject at hand. It explains the scope of this work and its related subjects.

The power of simulations and predictions are discussed with their advantages and limitations. A good insight into the finite element method is given in conjunction with real life applications of engineering continuum problems.

The second chapter is the review of the literature, where the author conducted a thorough research of available unclassified material on the thesis subject. It introduces the few leading useful military sponsored researches. It discusses their accomplishments, their advantages, limitations, and their relation to this work.

The third chapter deals with the structural loading boundary conditions and material properties. The geometric dimensions of the laminated composite panel and its loading boundary conditions are configured and explained. The experimental critical, buckling and failure loads from NRL are given here. The composite stress analysis in laminated composites is explained together with a sketch of the ply orientation and staking of the laminate matrix. Also given is the ply lay-up and thicknesses, together with the material mechanical properties.

The fourth chapter explains the thermal boundary conditions where the laser beam geometry and energy are specified, together with the thermal properties. The material degradation thermal relations of strength, modulus, density, specific heat, and conductivity are shown in graphical forms.

The fifth chapter describes the modeling and the finite element formulation of the problem. The initial considerations and the development

plan of attack for the solution of the problem is given there. The basic fundamentals of the finite element method as applied to the model for subdivision and transformation are given. The three-dimensional finite element model of the problem is drawn and shown. The theory of the composite shell element is introduced together with its elastic constants, stress, strain, stiffness, buckling, and load/strain relationship. Also, in this chapter the Galerkin finite element formulation of the general energy equation is given considering conduction, convection, and radiation. The solutions were shown for linear steady state, linear transient, and non-linear transient. Equilibrium iterations to approach the correct solution were explained together with the convergence criteria.

The sixth chapter presents the analysis and results. Here all the relevant input and output data is displayed for both the stress buckling modes and the heat transfer analysis together with the subsequent thermal loads, contours, and other parameters are shown. They are indicative, successful, accurate, and, perhaps, impressive.

The seventh chapter contains the discussion, conclusions, and suggestions for further work. The discussion explains the analysis and validates the results. The conclusions are summarized in accordance with the flow of the chapters. The suggestions for further work indicate the possibilities of improvements, other applications to be tackled, and experimentation requirements.

CHAPTER 2

REVIEW OF THE LITERATURE

The author has conducted deep and thorough computerized research of the existing unclassified literature on this thesis subject in the United States, Europe, and the Soviet Union. However, since published knowledge in both Europe and the Soviet Union seems to be primitive, only the leading few useful military sponsored U.S. research documents are reviewed here. These documents are primarily concerned with laser-induced damage experiments and/or simulations to aircraft or missiles, in conjunction with/without laminated composites, and vice versa. This chapter discusses those publications accomplishments, advantages, shortfalls, limitations and their relation to the work contained in this thesis.

Sheryl K. Bryan, a United States Air Force (USAF) Aerospace Engineering officer, conducted research that lead to her degree of Master of Science in 1983.[21] The research subject was a reanalysis method for

[21]Sheryl K. Bryan, "Reanalysis Methods for Structures with Laser-Induced Damage" (Unpublished MS Thesis, Air Force Inst. of Tech., Wright-Patterson AFB, Ohio, 1983), pp. 1-103.

structures with laser-induced damage. Strength analysis of a structure which has encountered a laser strike was developed. The method accounted for three types of laser-induced damage:

1. Loss of structure due to melting,
2. Change of material properties due to temperature changes, and
3. Addition of load due to thermal stress.

The program used heat balance calculations over successive finite time increments on an array of finite elements bisecting the laser beam spot to determine the temperature distribution. Those results were then converted to structural stiffness parameters and the structural analysis was performed using a finite element based reanalysis method, which predicted the damage effects from the initial undamaged solution. The researcher claimed that the program gave agreement with results obtained from a separate analysis. No comparison of the program results with experimental data was done. Material used was isotropic aircraft metal and not a composite. Buckling was not considered and the heat conduction solution was two-dimensional.

Laser-target interaction and blast wave formation in DNA/NRL laser experiment was numerically simulated by a team of researchers in 1986.[22] They presented details of a one-dimensional numerical simulation code intended to model the laser equipment in high pressure. The one-dimensional

---

[22]U.S. Department of the Navy, Numerical Simulation of the Laser-Target Interaction and Blast Wave Formation in the DNA/NRL Laser Experiment, by John L. Giuliani and Margaret Mulbrandon, Memorandum Report 5762 (Washington, D.C.: Geophysical and Plasma Dynamics Branch, Plasma Physics Division, Naval Research Laboratory, 1986), pp. 1-56.

code cannot model instabilities development, self-generated magnetic fields, or hysteresis losses. The results indicated unrealistically large amounts of radiation loss.

A high-order theory for geometrically non-linear analysis of composite laminates was presented in 1987.[23] The two researchers developed a refined, third order laminate theory that accounted for transverse shear strains. Their theory allowed parabolic description of the transverse shear stresses, and hence the shear correction factors of the usual shear deformation theory were not required. This theory also accounted for small strains with moderately large displacements (i.e. Von Karmen strains). They derived closed-form solutions of the linear theory for certain cross-ply and angle-ply plates and cross-ply shells. The finite element model was based on independent approximations of the displacements and bending moments (i.e. mixed formulations), and therefore only zero continuity approximations were required. The mixed variational formulations they developed suggested that the bending moments could be interpolated using discontinuous approximations (across inter-element boundaries). They used the finite element method in order to analyze cross-ply and angle-ply laminated plates and shells for non-thermal stress bending and for natural vibration. This

[23]J. N. Reddy and C. F. Liu, A Higher-Order Theory for Geometrically Nonlinear Analysis of Composite Laminate, NASA Contract Report 4056 (Blacksburg, VA: Virginia Polytechnic Institute and State University, 1987), pp. 1-99.

theory, however, fell short of catering for non-linear material or thermal loading.

Elastic wave dispersion in laminated composite plate was studied by a group of researchers in 1987.[24] They examined the dynamic behavior of infinite periodically laminated medium using the stiffness method that they have developed previously. They concentrated on studying dispersion of waves in a laminated plate. In their approach each lamina was divided into several sublayers and the displacement distribution through the thickness of each sublayer was approximated by polynomial interpolation functions in such a way that displacements and tractions were continuous across the interfaces between adjacent sublayers. This study was motivated by the desire to model wave propagation in a continuous fiber-reinforced laminated plate. The deduction was that if the wavelength is long compared to the fiber diameters and spacing, then each lamina can be modeled as a homogeneous transversely isotropic medium with the symmetry axis parallel to the fibers. The overall effective elastic properties of such a medium could be calculated from the fiber and matrix properties by using an effective modulus theory developed in 1964. Such an assumption has been made in their paper. Thus the dispersion characteristics of guided waves in a layered anisotropic plate was studied by them. In the analysis they assumed that each lamina is transversely isotropic with the symmetry axis aligned with either the x-axis or the y-axis. This

[24]S. K. Datta, et al. Elastic Wave Dispersion in Laminated Composite Plate, Contract N00014-86-K-0280, (Bolder: University of Colorado, 1987), pp. 1-8.

assumption was not necessary for the development of the equations, but it was made to keep the algebra as simple as possible for the anisotropic problem they had. The results gave good approximation to experimental values. Neither a static nor a thermal loading were used.

Funded by the Department of Energy, Washington, D.C., Mr. Vincent Prantil, a researcher in the structural mechanics division of Sandia Labs., Livermore, conducted a research on the response of a thin cylindrical shell under lateral impulse loads in 1988.[25] In support of investigating the lethality levels of short pulse width lasers, this combined analytical/experimental program was underway in Sandia National Laboratories to predict large deformation response of conceptual ballistic missile designs to impulsive loading. Both unpressurized and pressurized cylindrical shell models have been analyzed and tested. The type of impulsively loaded metal structures in question exhibit large scale plastic deformation and local dynamic pulse buckling instability which subsequently influence the loaded surface collapse. Impulse loads were simulated using both lead spray and light initiated high explosive techniques. Finite element calculation using a modified form of the Hughes-Liu shell element based on a modified code of the DYNA3D package verified several characteristics of the structural response observed by the researcher in experiments. The role of the computational results in identifying lethal impulse levels and response nodes

[25]V. C. Prantil, Response of a Thin Cylindrical Shell Under Lateral Impulse Loads (Livermore: Structural Mechanics Division, Sandia National Laboratories, 1988), pp. 1-75.

were described. In addition, the requirements for initial imperfections and fine mesh discretization for those problems were discussed.

The laser weapon/target interaction exhibited three characteristic response time regimes which were treated separately. The characterization of the full response was broken down into:

1. Surface physics response,
2. The one-dimensional shock wave response,
3. The overall global structural response.

The surface physics addressed the relationship between weapon output and the compressive shock wave imparted to the target surface. In an x-ray laser encounter, the weapon output impinged on the target surface. The radiant energy absorption often resulted in melting of the exposed target skin and plasma blow off, delivering a compressive shock wave into target. This exchange took place in a submicrosecond time span. The response of the one-dimensional shock wave, (also called material or hydrodynamic response) was concerned with several effects. Most important of these effects was the possibility of the material spallation due to the interaction of stress waves in the material. There was also the possibility of material degradation due to the short intense compressive shock wave introduced during load delivery. The response was characterized by the time over which the resulting stress waves propagate through the shell aluminum alloy metal wall, imparting a residual momentum in the target. Such effects occur on microsecond time scales for the

target materials of interest. Finally, the structural response described the overall target deformation occurring over times of several milliseconds and beyond. Within this last time frame, the entire structure is responding to the applied load. This is exactly what we are trying to analyze in this thesis, but for laminated composites instead of aluminum alloys. The researcher investigates and describes his analytical effort to capture the essential aspects of the structural response modes. In doing so probable relevant failure mechanisms could have been identified. Also the computational capability of non-linear large deformation finite element codes could have been verified, in addition to predicting the observed behaviors in the accompanying experiments. Predicting material failure, however, has not been attempted by the researcher, and actual use of laser was not experimentally attempted.

Failure of mechanically loaded laminated composites subjected to intense localized heating was examined by Dr. Ronald Gularte and his research team in the NRL, Washington, D.C., in 1987.[26] They presented a numerical procedure for predicting failure in laminated composites subjected to simultaneous intense localized heating and applied mechanical loads. Their method consisted of a non-linear, axisymmetric, two-dimensional finite difference thermal analysis including the effects of surface ablation, as well as the radiation losses, convection losses, and temperature dependent

[26]Ronald C. Gularte et al., "Failure of Mechanically Loaded Laminated Composites Subjected to Intense Localized Heating," International Journal for Numerical Methods in Engineering, Vol. 25 (London: Wiley and Sons Ltd., 1988), pp. 561-570.

thermophysical properties. They used their results in conjunction with a flat plate finite element code to predict the failure of laminated composites. Predictions based on the numerical analysis were compared with experimental results obtained from mechanically loaded graphite epoxy coupons spot-irradiated at various intensities.

The approach presented consisted of the integration of a high temperature material property data base with non-linear thermal analysis capability to produce a spatial and temporal temperature distribution within an intensely locally heated structure which, in turn, was used in the mechanical code to predict structural failure. The thermal degradation of material properties resulted in material non-linearities. We conclude that the overall strategy adopted in the above mentioned research to be considered as an uncoupled iterative procedure between a stress model and a thermal model. The model used was two-dimensional, and the experimental irradiated specimen used was tensile rather than compression loaded. There were some agreements, but, there were some disparities in the analysis which the researchers attributed to the slight inaccuracies in the thermal calculations which may have lead to errors in defining the temperature-dependent mechanical properties. They added, that the use of classical plate theory to model the complex stresses state in the vicinity of degraded material could have been an over-simplification.

An analytical model based on the sublaminate approach and fracture mechanics was developed[27] to study the growth of delamination. This report analyzed the inter-laminar fracture in composites under combined loading. Plane strain conditions were assumed and estimates were provided for the total strain energy release rate and modes contributions. The energy release rate estimated were used in combination with experimental data on graphite/epoxy laminates. Reasonable agreement was demonstrated for the range were the experimental observations indicated transverse crack tip delamination to be the predominant failure mode. The analytical model was two-dimensional, and the assumptions of plane strain conditions with negligible thickness strain are over-simplification. No thermal analysis was done.

A final technical report describing the research done on damage models of continuous fiber composites was introduced by Mr. D.H. Allen, Aerospace Engineering Department, Texas A&M University in 1988.[28] This report was submitted to the Air Force Office of Scientific Research, USAF. The report summarized research completed during a four year period under USAF grant. The objective of the research has been to develop an accurate damage model for predicting strength and stiffness of continuous fiber laminated

---

[27]Erian A. Armanios, Analysis of Interlaminar Fracture in Composites Under Combined Loading (Atlanta: Georgia Institute of Technology, 1988), pp. 1-30.

[28]David H. Allen, Research on Damage Models for Continuous Fiber Composites, Final Technical Report (College Station, Texas A & M, 1988), pp. 1-86.

composite media subjected to fatigue or monotonic loading and to verify this model with experimental results obtained from composite specimens of selected geometry and make-up. The work performed was in four parts:

1. Development of the constitutive equations relating stresses to strains and damage internal state variables which might have been used in a stress gradient field,
2. Development of internal states variables growth laws as a function of load history for matrix cracking, interlaminar fracture, etc.,
3. Development of finite element algorithms capable of evaluating ply properties in damaged components,
4. Perform experiments on components with selected stacking sequences in order to verify the model.

On the basis of the experimental studies, a general framework was developed using continuum damage mechanics to characterize the response of laminates with matrix cracks. This model was compared favorably with experimental evidence. The model was then extended to account for both matrix cracks and delaminations, and compared favorably with experimental results. The analyses were all two-dimensional, and no thermal effects or loading were introduced. This research concentrated on the micro-structural damage rather than the overall or macro-structural damage which is of engineering design interest to us.

An interim report on the development of a progressive failure model for strength of laminated composite structure was composed by P.Y. Tang, for the Naval Ocean Systems Center, San Diego in 1989.[29] The researcher deduced that the various progressive failure schemes/models results do not compare satisfactorily with experimental data when geometrically complicated laminated composite specimens are in question. The researcher proceeded with an assumption based on the introduction of an improved ply failure criterion into the progressive failure model should improve the accuracy of predicting the strength of laminated composite structure. The improved version of the finite element package COSMIC/NASTRAN of NASA is proposed to be used, in conjunction with a Stanford University package called PDHOLE which was specially written to predict the tensile strength of a composite laminate strip containing an open hole. This proposal by the above mentioned researcher is to take place in the fiscal years 1990-91 timeframe to try and prove the researcher assumption. No thermal loading were considered, and the proposed modeling is in two-dimensions.

Compression failure mechanics in unidirectional composites was studied in a NASA technical memorandum.[30] Possible failure modes of

---

[29]P. Y. Tang, Development of a Progressive Failure Model for Strength of Laminated Composite Structure (San Diego: Naval Oceans System Center, 1989), p. 2.

[30]H. Thomas Hahn and Jerry G. Williams, Compression Failure Mechanics in Unidirectional Composites, NASA Technical Memorandum 85834 (Langley, VA: NASA, 1984), pp. 1-26.

constituent material were summarized and analytical models were reviewed. The composites used were unidirectional and no heating was used.

The buckling modes and failure characteristics of differently stiffened composite shear panels were described in NASA Technical Memorandum 2153.[31] Shear stress-strain at tow temperatures were compared with linear buckling analysis and failure behavior is discussed.

[31]Mark J. Stuart and Jane A. Hagman, Buckling and Failure Characteristics of Graphite-Polyimide Shear Panels, NASA Technical Memorandum 2153 (Langley, VA: NASA, 1983), pp. 1-21.

CHAPTER 3

STRUCTURAL LOADING BOUNDARY CONDITIONS AND MATERIAL PROPERTIES

In this chapter the structural loading boundary conditions are inscribed and material properties are stated. The geometric dimensions of the laminated composite panel and its loading boundary conditions are configured and explained. The experimental critical, buckling and failure loads from the NRL are given here. The composite stress analysis in laminated composites is explained together with a sketch of the ply orientation and staking of the laminate matrix. Also given is the ply lay-up and thicknesses, together with the material mechanical properties.

As we discussed in the introduction we would like to predict the buckling and post-buckling behavior of heated flat laminated composite rectangular orthotropic compression panels with edges rotationally restricted. A good example of one particular application for such a high temperature, low-weight material is the aft body of the Space Shuttle.

Loading Boundary Conditions:

t = 0.1144

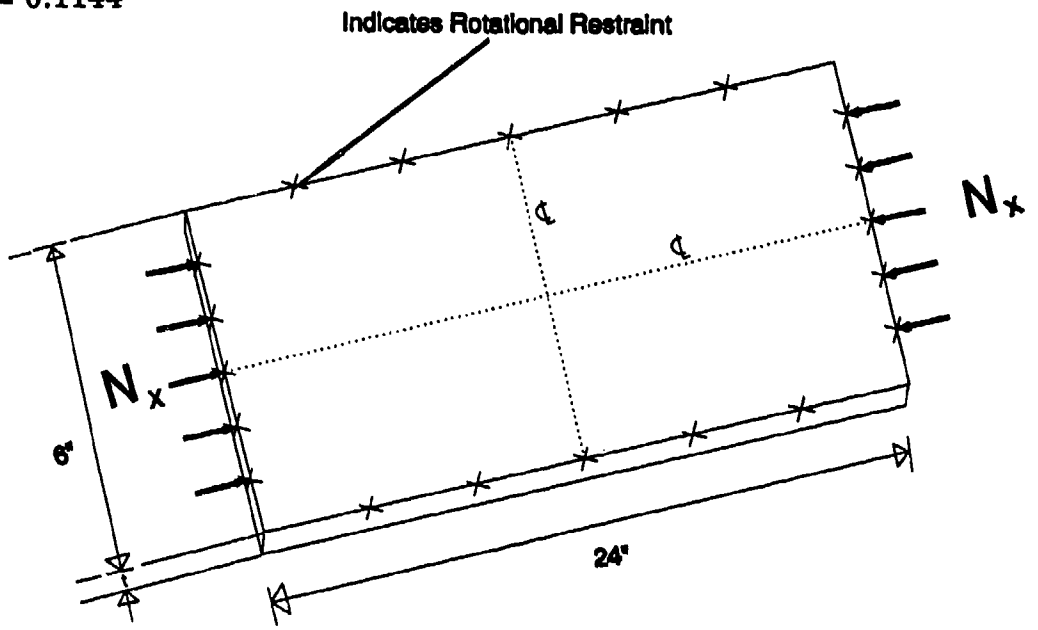

Figure 3.1 Loading Boundary Conditions

(*) N_x-Critical	N_x-Buckled	N_x-Failure
2410 lb/in	3927 lb/in	5130 lb/in

COMPOSITE STRESS ANALYSIS:

A lamina (ply), as shown in figure 3.2(a), is a flat, sometimes curved as in a shell, arrangement of unidirectional fibers or woven fibers in a matrix. A laminate, as shown in figure 3.2(b), is a stack of laminae with various orientations of fiber directions called ply orientations in the laminae.[32]

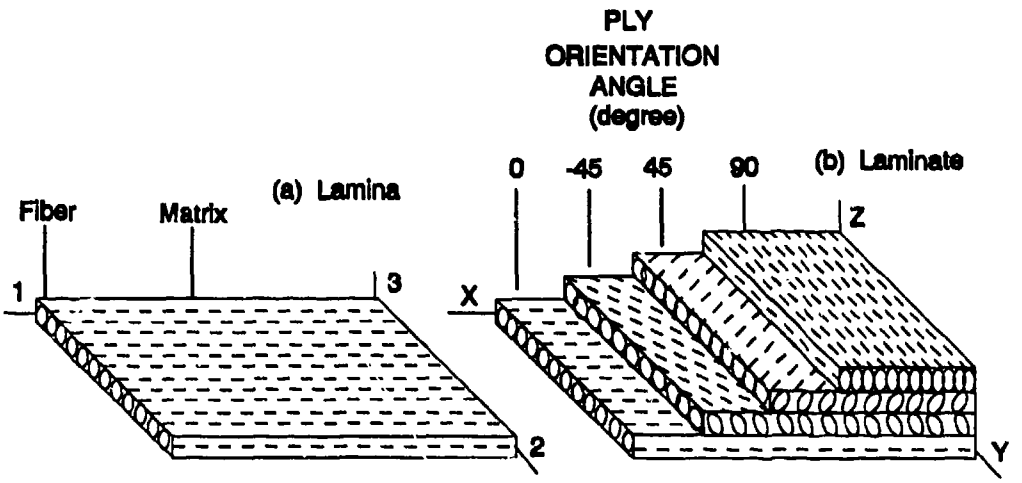

Figure 3.2 Laminated Composite

Due to the inherent heterogeneous nature of fiber-reinforced composite materials, they are studied in both micromechanics and macromechanics. In the first, composite material behavior is studied by examining the interaction of the constituent fibers and matrixes on a microscopic scale. In macromechanics, composite material behavior is studied

[32]P. Y. Tang, Development of a Progressive Failure Model for Strength of Laminated Composite Structure, p. 2.

by presuming the material to be homogeneous and detecting the effect of the constituent material to meet a particular structural requirement.[33] This latter study is what is important to us in this work, from the engineering design point of view.

[33]Ibid, p. 2.

PLY LAY-UP:

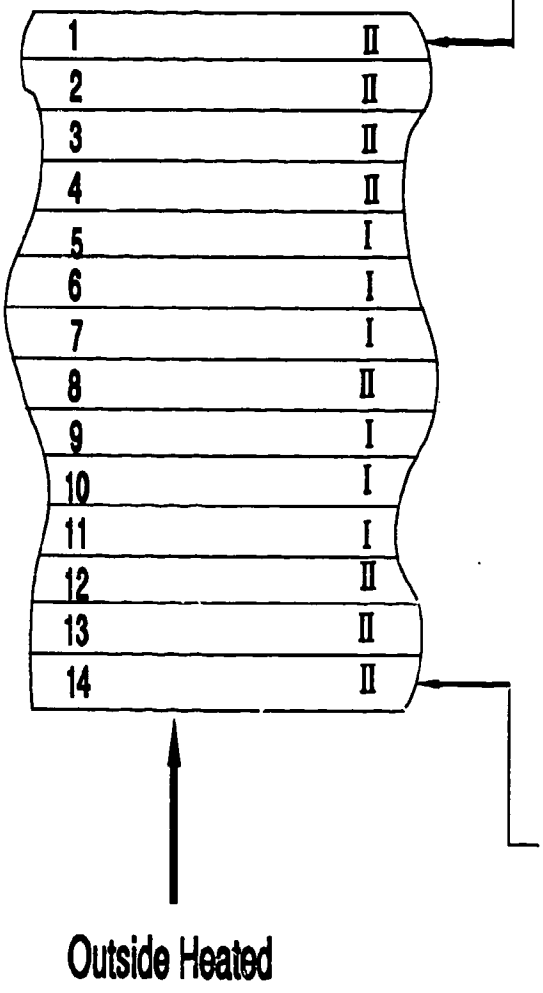

PLY NO.	ORIENTATION	TYPE
1	45 Deg.	II
2	-45 Deg.	II
3	0 Deg.	II
4	-22 Deg.	II
5	0 Deg.	I
6	45 Deg.	I
7	-45 Deg.	I
8	90 Deg.	II
9	-45 Deg.	I
10	45 Deg.	I
11	0 Deg.	I
12	0 Deg.	II
13	-45 Deg.	II
14	45 Deg.	II

WHERE:

TYPE	I	0.0052"	PREPREG
TYPE	II	0.0104"	PREPREG

MATERIAL PROPERTIES:

Graphite/Epoxy

Hercules AS4/3501-6

MECHANICAL PROPERTIES	Units	Type AS4 Fiber	AS4/3501-6 Composite
Tensile Strength	Ksi	520	315
0 Degree Direction	MPa	3,587	2,170
Tensile Modulus	Msi	34	21
0 Degree Direction	GPa	235	145
Short Beam Shear:			
Strength	Ksi	____	18.5
Unidirectional	Mpa	____	128
Flexural Strength	Ksi	____	260
Unidirectional	Mpa	____	1,793

Compression Strength at room temperature is: 64 Ksi

INTER-LAMINAR SHEAR:

At Room Temperature	7.3 Ksi
At 200 Degrees F	8.8 Ksi

GEOMETRIC CONSIDERATIONS:

In order to reduce the computing time, effort and cost, only a quarter of the laminated composite panel was considered to be modeled (upper right section) due to symmetry. In addition, the material properties were such that the quadrant or $\pi/2$ modeling is more than adequate within the engineering bounds of the study, as opposed to detailed complete circle/panel modeling.

The uniformity and circumference accuracy of the laser beam incident circle on the panel is adequate for engineering design purposes.

CHAPTER 4

THERMAL BOUNDARY CONDITIONS

The thermal boundary conditions together with the laser beam geometry and energy are specified in this chapter. Also stated are the material thermal properties. The material degradation thermal relations of strength, modulus, density, specific heat and conductivity are presented graphically.

CASE	SPOT SIZE/RADIUS (in)
1	1.000
2	2.000
(*)3	3.000

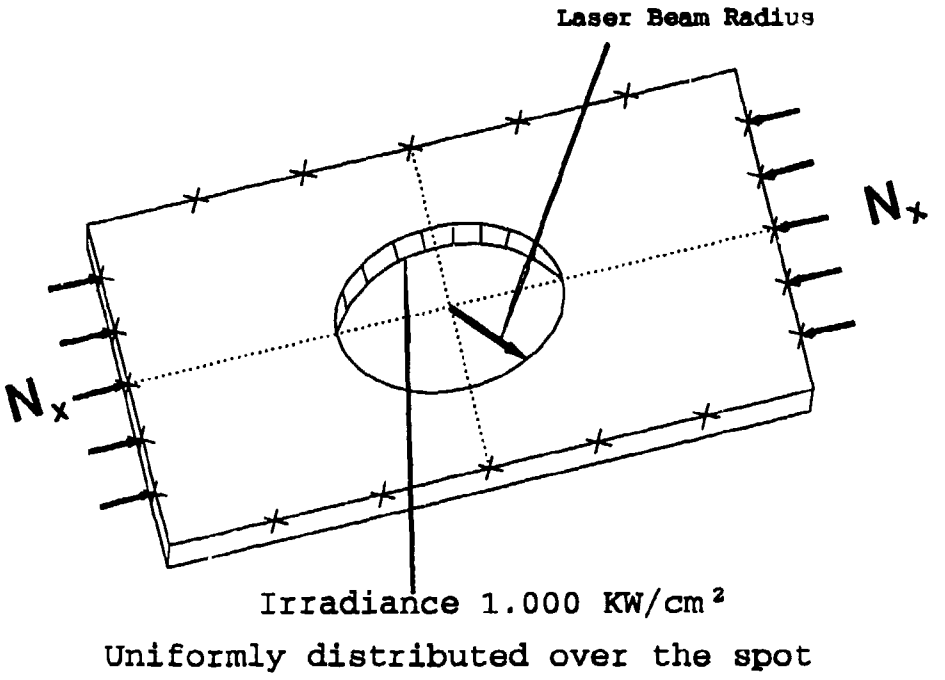

Figure 4.1 Irradiation Boundary Conditions

The degradation of the room temperature properties with increasing temperature is given in the following next five figures/graphs. The first graph shows Ultimate Strength (% R.T. value) against Temperature (Deg. R), while the second graph shows Modulus (% R.T. values) against Temperature (Deg. R), the third, fourth, and fifth graphs show the temperature-dependent density, specific heat, and conductivity of graphite/epoxy.[34]

[34]Ronald C. Gularte, Head, Engineering Materials Group, Naval Research Lab., and G. Holderby, Wright Research and Development Center, Washington, D.C., private communications, 1990-1991.

THERMAL PROPERTIES	UNITS	TYPE AS4 Fiber	AS4/3501-6 Composite
Specific Heat, C			
(RT)	J/G.Deg.K	0.92	3.1
	Btu/h.ft.Deg.F		
	or: Cal/g Deg.C	0.22	0.74
Thermal Conductivity, K			
0 Deg. direction			
(RT)	Btu/h.ft.Deg.F	15	2.65
	Watt/M Deg.K	26	4.60
90 Deg. direction			
(RT)	Btu/h.ft.Deg.F	---	0.36
	Watt/M Deg.K	---	0.62

We are going to limit ourselves to one Loading and One Heating Condition as indicated by (*) in text in Chapters (3,4).

N_x (Critical) = 2410 lb/in, N_x (Buckling) = 3927 lb/in

A (6") Spot Diameter with an Irradiance of (1.000 KW/Sq.cm)

THERMAL CONSIDERATIONS:

Both ablation and spall at the interfaces of the laser beam circle on the panel were neglected due to the fact that the temperature generated in this exercise does not bring the panel to these stages. This was set by the (NRL), however, it is possible to include the effect of both readily in the program should this be required. The instantaneous damage that takes place in the panel is due to mechanical buckling rather than anything else. If elevated temperature causing spalling and ablation are reached then the effect of both would be secondary, since the structural buckling damage would have already took place.[35]

The effect of air flow and painting on the surface to resemble real life helicopter outer panel situation were both examined. The effect of both are trivial due to the speed of the heating process.[36,37]

---

[35]Bryan, "Reanalysis Methods for Structures with Laser-Induced Damage," pp. 48-70.

[36]Ibid, pp. 48-70.

[37]Prantil, "Response of a Thin Cylindrical Shell Under Lateral Impulse Loads," pp. 51-58.

PROPERTIES DEGRADATION WITH INCREASED TEMPERATURE

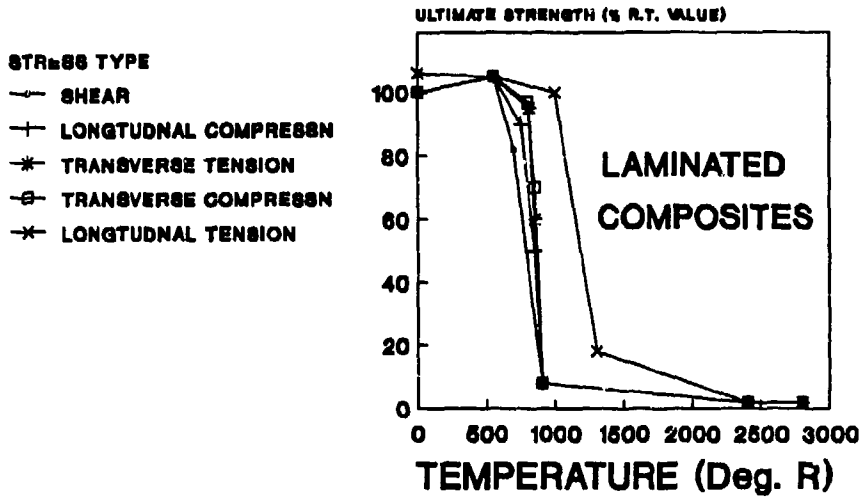

LASER INDUCED DAMAGE

Figure 4.2 Properties Degradation (1)

PROPERTIES DEGRADATION WITH INCREASED TEMPERATURE

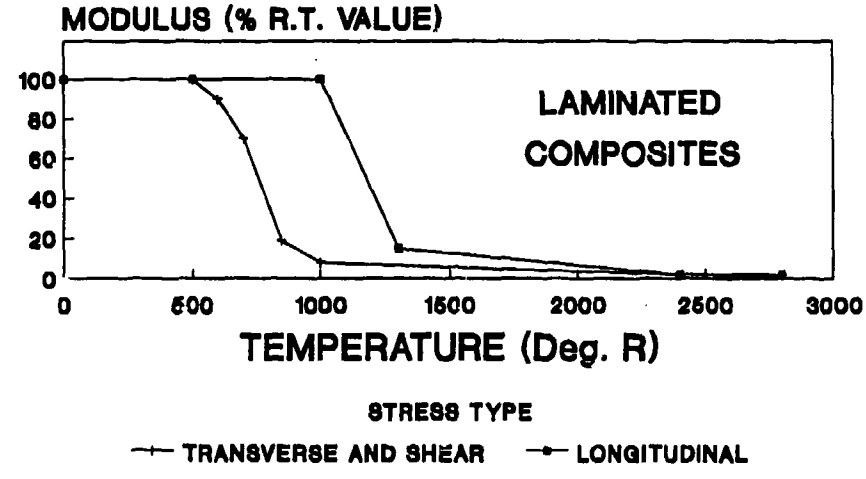

LASER INDUCED DAMAGE

Figure 4.3 Properties Degradation (2)

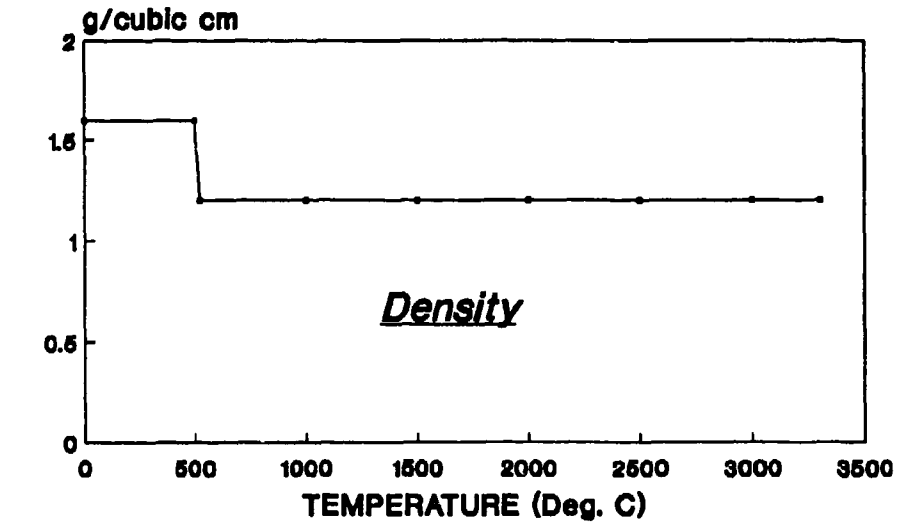

Figure 4.4 Temperature Dependent Density of Composites

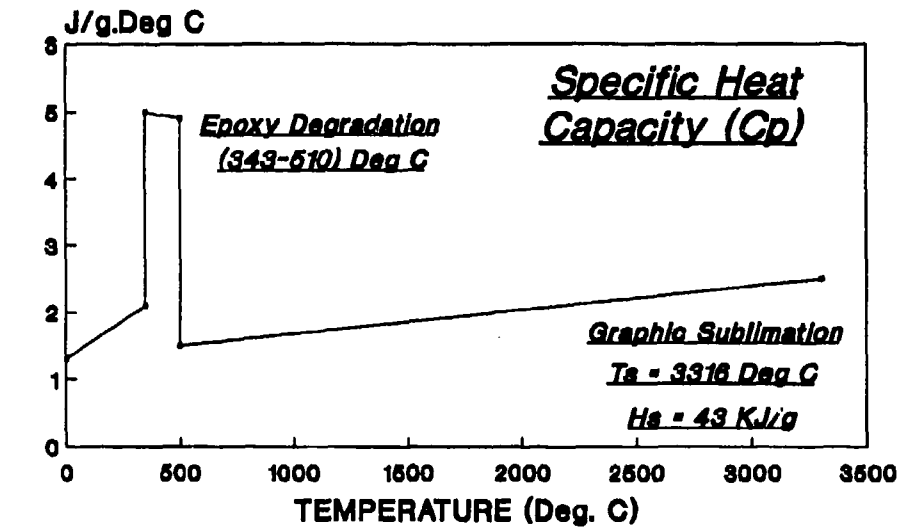

Figure 4.5 Temperature Dependent Specific Heat of Composites

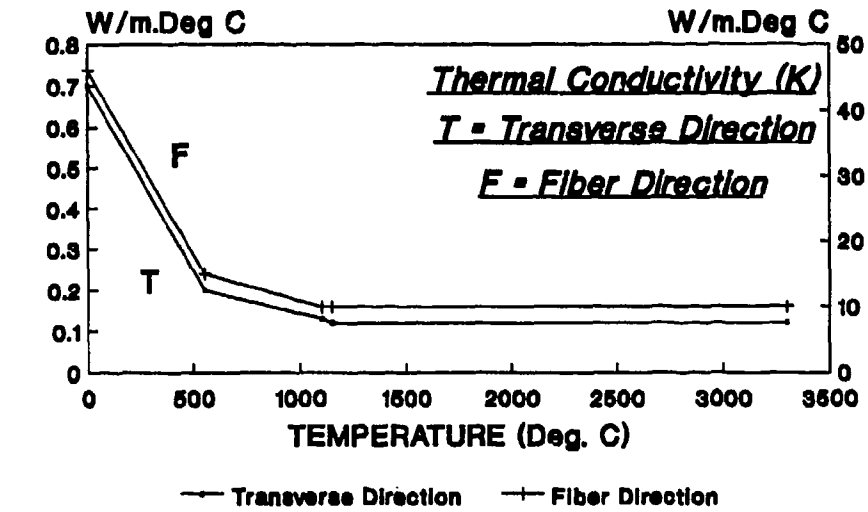

Figure 4.6 Temp. Dependent Thermal Conductivity of Composites

CHAPTER 5

MODELING AND THE FINITE ELEMENT FORMULATION OF THIS PROBLEM

The modeling and the finite element formulation of this thesis problem are presented in this chapter. The initial considerations and the development plan of attack for the solution of the problem are given here. The basic fundamentals of the finite element method as applied to the model subdivision and transformation is given. The three-dimensional finite element model of the problem is drawn and shown. The theory of the composite shell element is introduced together with its elastic constants, stress, strain, stiffness, buckling, and load/strain relationships. Also, in this chapter the Galerkin finite element formulation of the general energy equation is given considering conduction, convection and radiation. The solutions were shown for linear steady state, linear transient, and non-linear transient. Equilibrium iterations to approach the correct solution were explained together with the convergence criteria.

In order to be able to capture all the influencing behavior in this complicated set-up of both stress and temperature distribution dynamic

dependence on material properties, the author chose to work in three-dimensions for both the stress and thermal analysis. The three-dimensional finite element mesh used to model the current problem is shown on the next page. Since the geometrical configuration of the laminated composite panel in question is symmetrical in all three cartesian coordinate axis, obviously, only quarter of the panel is modeled. However, the initially suggested[38] development plan of attack for the solution of the problem was only in two-dimensions and is as follows:

1. To conduct an analysis to verify that N_x-Critical is indeed the critical buckling load.
2. Perform a simplified (axi-symmetrical or one-dimensional) thermal analysis which should result in the temperature distribution as a function of time.
3. Finally, use the thermal results as input to the incipiently critically loaded model and determine the amount of time required to initiate buckling.
4. If, time allows, one could use the previous approach on the post-buckled panel to predict the time required to fail the irradiated panel.

The basic fundamental of the finite element method is the sub-division of the domain of interest into smaller bounded subdomains called

[38]Gularte and Holderby, Private communications.

elements. Such elements are connected together at discrete points on their extremities called nodes.

The behavior of a dependent variable over each element may be approximated by continuous functions such that at points X,Y,Z:

$$\phi(X,Y,Z) = \sum_{i=1}^{n} N_i(X,Y,Z)\phi_i \tag{5.1a}$$

where n is the number of elemental nodes. Similarly derivatives may be expressed, typically:

$$\frac{\partial \phi}{\partial X}(X,Y,Z) = \sum_{i=1}^{n} \frac{\partial N_i}{\partial X}(X,Y,Z)\phi_i \tag{5.1b}$$

In the finite element method N(X,Y,Z) are referred to as the shape (or interpolation) functions. These are generally cast in a parametric form using an (ξ,η,ζ) coordinate system,[39] and in continuum mechanics are chosen to ensure functional continuity at element boundaries. However, such continuity need not exist for function derivatives, these elements are referred to as (Co) continuous.

The transformation of derivative terms from parametric to the physical coordinate system is obtained by the chain rule and by invoking equation (5.1b), typically:

$$\frac{\partial X}{\partial \xi} = \sum_{i=1}^{n} \frac{\partial N_i}{\partial \xi} X_i$$

[39]Zienkiewicz, "The Finite Element Method," pp. 132-256.

Then adopting matrix notation, in two dimensions:

$$\begin{bmatrix} \frac{\partial N_i}{\partial \xi} \\ \frac{\partial N_i}{\partial \eta} \end{bmatrix} = \begin{bmatrix} \frac{\partial X}{\partial \xi} & \frac{\partial y}{\partial \xi} \\ \frac{\partial X}{\partial \eta} & \frac{\partial Y}{\partial \eta} \end{bmatrix} \begin{bmatrix} \frac{\partial N_i}{\partial X} \\ \frac{\partial N_i}{\partial Y} \end{bmatrix}$$

i.e.

$$\begin{bmatrix} \frac{\partial N_i}{\partial \xi} \\ \frac{\partial N_i}{\partial \eta} \end{bmatrix} = |J| \begin{bmatrix} \frac{\partial N_i}{\partial X} \\ \frac{\partial N_i}{\partial Y} \end{bmatrix}$$

then

$$\begin{bmatrix} \frac{\partial N_i}{\partial X} \\ \frac{\partial N_i}{\partial Y} \end{bmatrix} = |J|^{-1} \begin{bmatrix} \frac{\partial N_i}{\partial \xi} \\ \frac{\partial N_i}{\partial \eta} \end{bmatrix} \tag{5.2}$$

When the dependent variable is interpolated at the same nodes as the dependent variables (X,Y,Z coordinates) the element is said to be isoparametric. When the dependent variable is interpolated at fewer nodes, the element is described as superparametric. Some typical element geometries are shown in Figure 5.1. Further information concerning the elements type, shape functions, continuity, compatibility, etc., can be found in "The Finite Element Method."[40]

[40]Ibid, pp. 132-256.

The three-dimensional finite element model of the problem is shown in the next Figure 5.2. The convention for stacking sequence in local element coordinate and the temperature distribution across the thickness of the plate is shown for the composite shell element in Figure 5.3. The side view of the model used is comprised of 120 shell elements for each layer of the laminated composite panel quadrant.

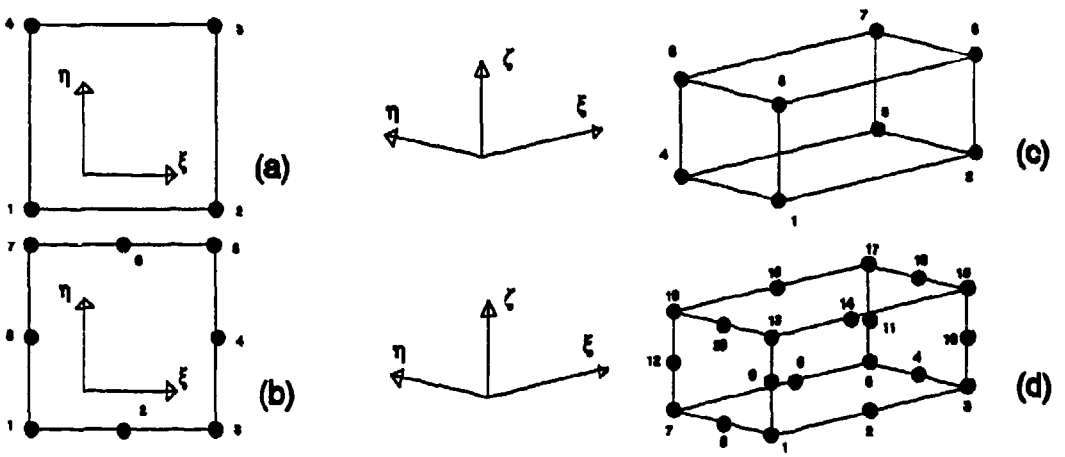

Figure 5.1 Element Types
(a) 2D Linear, (b) 2D Quadratic, (c) 3D Linear, (d) 3D Quadratic

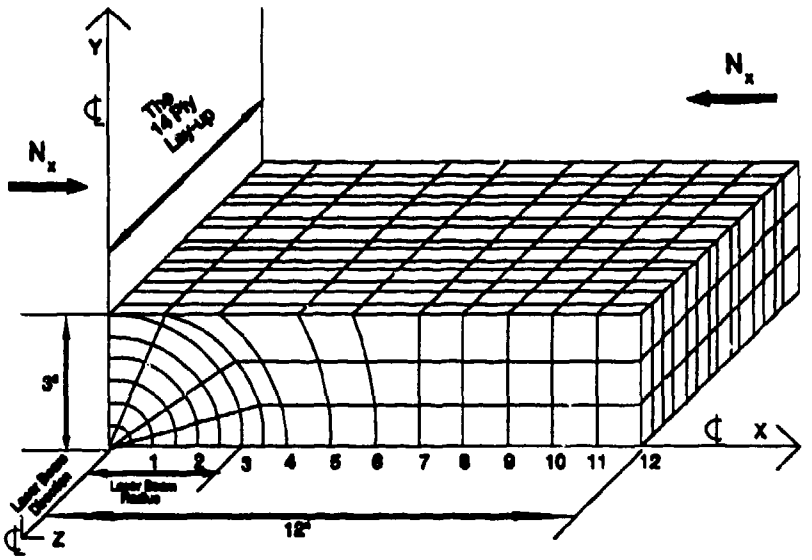

Figure 5.2 Three-dimensional Finite Element Model

5.1 COMPOSITE SHELL ELEMENT:

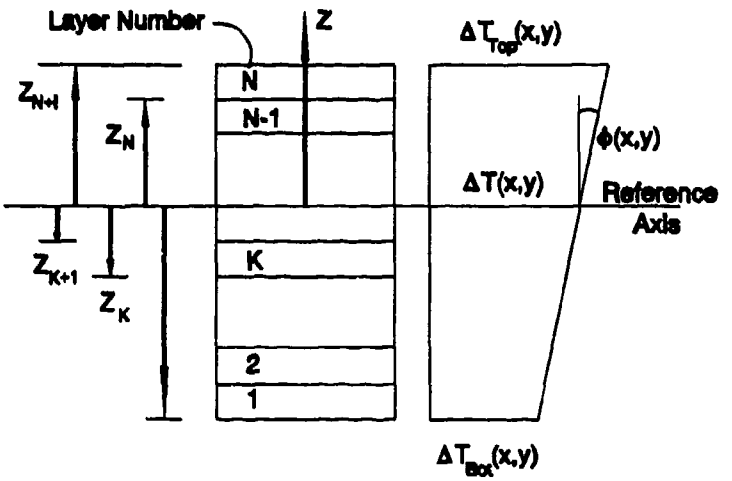

Figure 5.3 Composite Shell Element
Convention for stacking sequence in local element coordinate and the temperature distribution across the thickness of the plate

5.1.1 ELASTIC CONSTANTS:

Although for the most general cases of anisotropy the number of independent elastic constants is 21, these constants are required to define the general anisotropic material in pounds per square inch. This number is considerably reduced if the material internal composition possesses any kind of symmetry. A state of anisotropy possesses three mutually orthagonal planes of symmetry at each layer. If the reference system of orthagonal axes (X,Y,Z) is parallel to the principle material axes (1,2,3), and (z = 3) axis is perpendicular to the midplane of the structure at each point, the elasticity matrix D relating stress and strains is obtained as:

$$\begin{Bmatrix} \sigma_1 \\ \sigma_2 \\ \tau_{12} \\ \tau_{13} \\ \tau_{23} \end{Bmatrix} = \begin{bmatrix} D_1 & D_{12} & 0 & 0 & 0 \\ D_{12} & D_2 & 0 & 0 & 0 \\ 0 & 0 & D_3 & 0 & 0 \\ 0 & 0 & 0 & D_4 & 0 \\ 0 & 0 & 0 & 0 & D_5 \end{bmatrix} \begin{bmatrix} e_1 \\ e_2 \\ \gamma_{12} \\ \gamma_{13} \\ \gamma_{23} \end{bmatrix} \tag{5.3}$$

where γ equals shear stress, G equals shear modulus, and

$$D_1 = E_1/(1-\nu_{12}\nu_{21})$$
$$D_2 = E_2/(1-\nu_{12}\nu_{21})$$
$$D_{12} = E_2\nu_{12}/(1-\nu_{12}\nu_{21})$$
$$D_3 = G_{12}$$
$$D_4 = K_1 \times G_{13}$$
$$D_5 = K_2 \times G_{23}$$

the terms K_1 and K_2 are shear correction factors which are chosen to match the plate theory with certain classical solutions.[41]

If the principle axes of anisotropy 1, 2 do not coincide with the reference axes X, Y, but are rotated by a certain angle theta (θ), as illustrated in Figure 5.4 below:

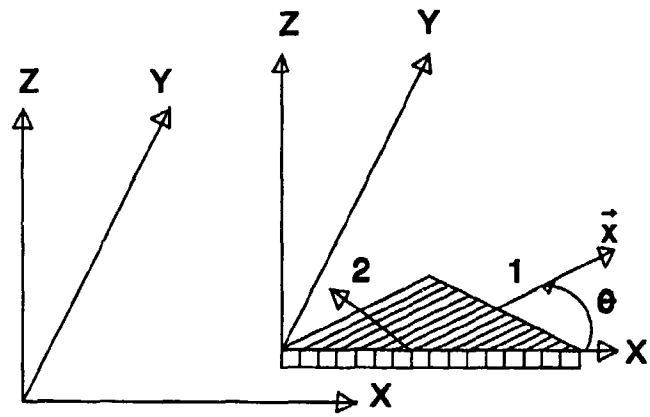

$\vec{x} = r_1 i + r_2 j + r_3 k$

$\vec{y} = s_1 i + s_2 j + s_3 k$

$\vec{z} = b_1 i + b_2 j + b_3 k$

$\vec{i}$, $\vec{j}$, $\vec{k}$ are unit vectors used to define a vector quantity in terms of its components.

$C = Cos\theta = r_1 b_1 + r_2 b_2 + r_3 b_3$

$S = Sin\theta = b_1 s_1 + b_2 s_2 + b_3 s_3$

b_1, b_2, b_3 are components of the z vector as s_1, s_2, s_3 and r_1, r_2, r_3 are components of the y and x vectors respectively.

Figure 5.4 Principle Axes of Anisotropy
Sign convention for principle in-plane material axes (1,2) and local element axes (X,Y)

[41]S. P. Timoshenko and J. M. Gere, Theory of Elastic Stability, 2nd Ed. (New York: McGraw-Hill, 1961), pp. 418-419.

The new elasticity matrix D is determined by the following transformation.

$$\begin{aligned} \sigma_{1,2,3} &= T\sigma_{x,y,z} \\ e_{1,2,3} &= T' e_{x,y,z} \end{aligned} \tag{5.4}$$

where

$$\begin{aligned} \sigma_{x,y,z} &= \{ \sigma_x, \sigma_y, \tau_{xy}, \tau_{xz}, \tau_{yz} \}^T \\ e_{x,y,z} &= \{ e_x, e_y, \gamma_{xy}, \gamma_{xz}, \gamma_{yz} \}^T \end{aligned} \tag{5.5}$$

$$T = \begin{bmatrix} T_1^T & 0 \\ 0 & T_2 \end{bmatrix}$$

and

$$T_1 \begin{bmatrix} C^2 & S^2 & SC \\ S^2 & C^2 & -SC \\ -2SC & 2SC & C^2-S^2 \end{bmatrix} \tag{5.6}$$

$$T_2 = \begin{bmatrix} C & S \\ -S & C \end{bmatrix} \qquad T' = \begin{bmatrix} T_1 & 0 \\ 0 & T_2 \end{bmatrix}$$

$$\begin{aligned} \sigma_{x,y,z} &= T^{-1}\sigma_{1,2,3} \\ &= T^{-1} D e_{1,2,3} \\ &= T^{-1} D T' e_{x,y,z} \\ &= \bar{D} e_{x,y,z} \end{aligned} \qquad \bar{D} = \begin{bmatrix} [Q_b]_{3\times3} & 0 \\ 0 & [Q_s]_{2\times2} \end{bmatrix}$$

where $[Q_b]$ is the bending part of the material matrix and $[Q_s]$ relates to the shear effects.

5.1.2 FORCE RESULTANT-STRAIN RELATIONSHIP:

The stress in the K^{th} layer in terms of the reference surface strains and curvature are:

$$\begin{Bmatrix} \sigma_x \\ \sigma_y \\ \tau_{xy} \end{Bmatrix}^K \quad [Q_b]^K \left[\begin{Bmatrix} e_{x^0} \\ e_{y^0} \\ \gamma_{xy^0} \end{Bmatrix} + Z \begin{Bmatrix} K_x \\ K_y \\ K_{xy} \end{Bmatrix} \right] \tag{5.7}$$

$$\begin{Bmatrix} \tau_{xz} \\ \tau_{yz} \end{Bmatrix}^K = [Q_s]^K \begin{Bmatrix} \tau_{xz} \\ \tau_{yz} \end{Bmatrix}$$

Stress resultants and stress couples can now be defined as those for homogeneous plate by integrating the above equations over each layer and summing the resulting expressions over the n plate layers.

$$N_x, N_y, N_{xy} = \sum_{k=1}^{n} \int_{Z_k}^{Z_{k+1}} (\sigma_x, \sigma_y, \tau_{xy})^{(K)} \, dz \tag{5.8}$$

$$M_x, M_y, M_{xy} = \sum_{k=1}^{n} \int_{Z_k}^{Z_{k+1}} (\sigma_x, \sigma_y, \tau_{xy})^{(K)} \, z dz$$

$$V_x, V_y = \sum_{k=1}^{n} \int_{Z_k}^{Z_{k+1}} (\tau_{xz}, \tau_{yz})^{(K)} \, dz$$

where Z equals the distance from the reference surface; N_x, N_y, and N_{xy} represent the in-plane shear forces; M_x, M_y, M_{xy} depict the in-plane normal and shear moments; and V_x, V_y, and V_{xy} portray the transverse shear forces. Carrying out the indicated integrations yields equation 5.9 listed below:

$$\begin{bmatrix} N_x \\ N_y \\ N_{xy} \\ \hline M_x \\ M_y \\ M_{xy} \\ \hline V_x \\ V_y \end{bmatrix} = \left[\begin{array}{ccc|ccc|cc} A_{11} & A_{12} & A_{13} & B_{11} & B_{12} & B_{13} & & \\ A_{21} & A_{22} & A_{23} & B_{21} & B_{22} & B_{23} & 0 & \\ A_{31} & A_{32} & A_{33} & B_{31} & B_{32} & B_{33} & & \\ \hline B_{11} & B_{12} & B_{13} & D_{11} & D_{12} & D_{13} & & \\ B_{21} & B_{22} & B_{23} & D_{21} & D_{22} & D_{23} & 0 & \\ B_{31} & B_{32} & B_{33} & D_{31} & D_{32} & D_{33} & & \\ \hline & & & & & & E_{11} & E_{12} \\ 0 & & & 0 & & & E_{21} & E_{22} \end{array}\right] \begin{bmatrix} e_x^0 \\ e_y^0 \\ \gamma_{xy}^0 \\ \hline K_x \\ K_y \\ K_{xy} \\ \hline \gamma_{xz} \\ \gamma_{yz} \end{bmatrix} \tag{5.9}$$

where

$$A_{ij} = \sum_{k=1}^{N} (QB_{ij})^K (Z_{k+1} - Z_k) \tag{5.10}$$

$$B_{ij} = \frac{1}{2} \sum_{k=1}^{N} (QB_{ij})^K (Z_{k+1}^2 - Z_k^2)$$

$$D_{ij} = \frac{1}{3} \sum_{k=1}^{N} (QB_{ij})^K (Z_{k+1}^3 - Z_k^3)$$

$$E_{ij} = \sum_{k=1}^{N} (QS_{ij})^K (Z_{k+1} - Z_k)$$

The presence of [B] above implies coupling between bending and extension. This term is equal to zero if the laminate is symmetric about the reference surface.

5.1.3 LOCAL ELEMENT STIFFNESS MATRIX:

The strain energy of the plate is given by:

$$\pi = \frac{1}{2}\iint \begin{Bmatrix} \epsilon^0 \\ k \\ \gamma \end{Bmatrix}^T \begin{bmatrix} A & B & 0 \\ B & D & 0 \\ 0 & 0 & E \end{bmatrix} \begin{Bmatrix} \epsilon \\ k \\ \gamma \end{Bmatrix} dxdy \tag{5.11}$$

which can be written as:

$$\pi = \frac{1}{2}\iint \begin{Bmatrix} \epsilon^0 \\ K \end{Bmatrix}^T \begin{bmatrix} A & B \\ B & D \end{bmatrix} \begin{Bmatrix} \epsilon^0 \\ k \end{Bmatrix} dxdy + \frac{1}{2}\iint \{\gamma\}^T \{E\} \{\gamma\} dxdy$$
$$- \frac{1}{2}\{U\}^T \left\{ \iint [B_b]^T \begin{bmatrix} A & B \\ B & D \end{bmatrix} [B_b] dxdy + \iint [B_s]^T [E] [B_s] dxdy \right\} \{U\} \tag{5.12}$$

where

$$\{U\}^T = \{ u_1, v_1, \theta_{z1}, u_2, v_2, \theta_{z2}, u_3, v_3, \theta_{z3}, w_1, \theta_{x1}, \theta_{y1}, w_2, \theta_{x2}, \theta_{y2}, w_3, \theta_{x3}, \theta_{y3} \} \tag{5.13}$$

$$[B_b] = \left[\begin{array}{c|c} [BP] & 0 \\ \hline 0 & [BB] \end{array}\right]_{6\times 18} \qquad [B_s] = \left[\begin{array}{c|c} 0 & [BS] \end{array}\right]_{2\times 18} \tag{5.14}$$

and [BP], [BB], and [BS] are the kinematic matrices.

[BP] and [BB] are partitioned matrices used for bending and [BS] is the same for shear.

The stiffness matrix is given by:

$$[K] = [Kb] + [Ks] \tag{5.15}$$

where

$$[Kb] \iint [Bb]^T \left[\begin{array}{c|c} A & B \\ \hline B & D \end{array}\right] [Bb]\, dx\,dy$$

$$[Ks] = \iint [Bs]^T [E]\, [Bs]\, dx\,dy$$

5.2 BUCKLING AND IN-PLANE FORCES:

When a structure is subjected to in-plane forces (i.e. forces that act tangent to a member axis or mid surface), membrane strain energy develops inside the structure. The effect of the membrane strain energy on the

total stiffness of structure is considered by adding the geometric stiffness matrix to the global stiffness matrix.

The geometric stiffness matrix is independent of elastic properties and depends only on element's geometry, displacement field and state of stress. It accounts for the effect of existing forces on the bending stiffness of structure.

In presence of membrane forces, the equation of static equilibrium:

$$[K]\{U\} = \{R\} \tag{5.16}$$

will change to:

$$[K + K_\sigma]\{U\} = \{R\} \tag{5.17}$$

where [K] is the stiffness matrix, $[K_\sigma]$ is the geometric stiffness matrix for the given load vector {R}, and {U} is the displacement vector.

As can be seen from the graph in Figure 5.6, representing the beam of Figure 5.5, the transverse displacement becomes very large and approaches infinity as the axial load approaches a certain limit. This limit, known as $P_{critical}$, is the buckling load for the structure.

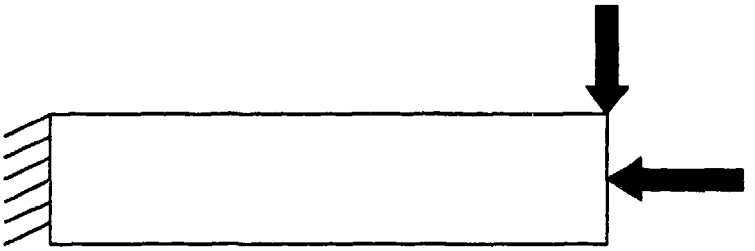

Figure 5.5 - Cantilever Beam

Buckling occurs when a member of the structure converts membrane strain energy into strain energy bending. After buckling, the member will usually fail because sudden large bending deformations are needed to store membrane energy. If the same problem is solved in the absence of the transverse loading shown in Figure 5.6, the load-displacement curve is obtained as in Figure 5.7.

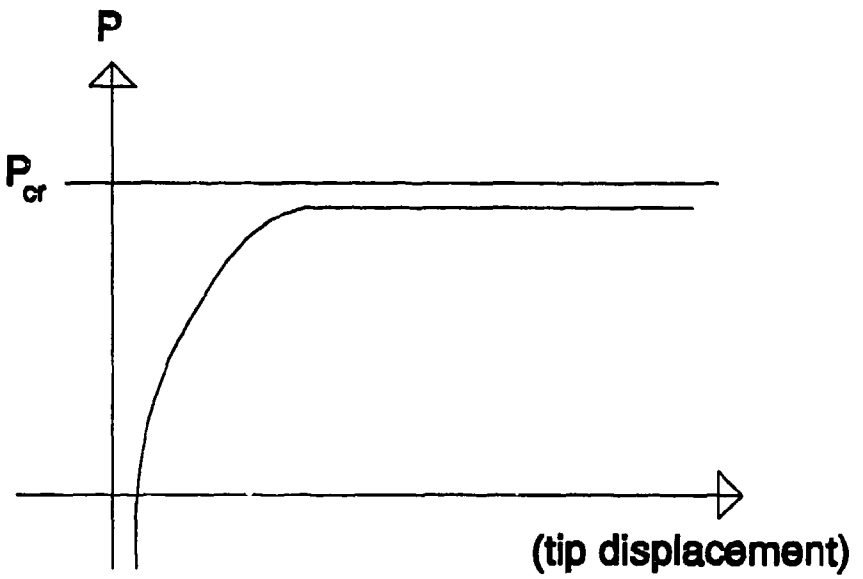

Figure 5.6
Load-displacement Curve for a Typical Beam/Column

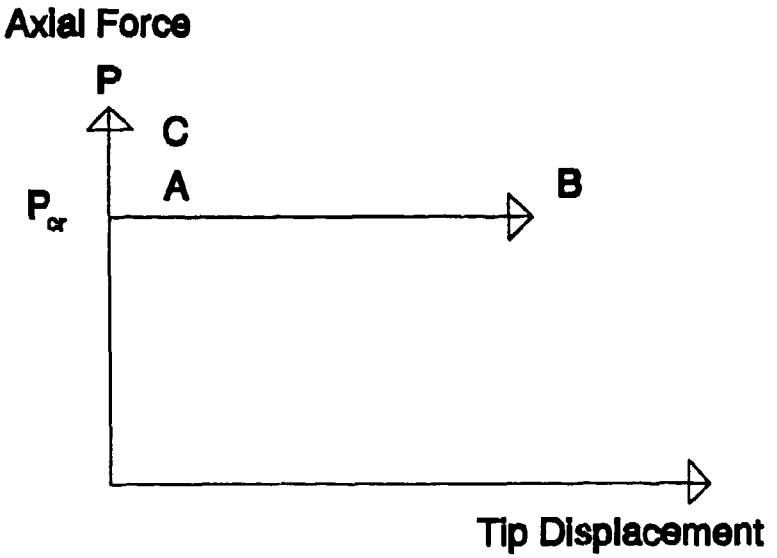

Figure 5.7
Load-displacement Curve for a "Perfect" Column

Note that in this case of Figure 5.7 above, the P_{cr} is a bifurcation point, after which two possible equilibrium configurations exist. In the post-buckling state, path AC of the above Figure 5.7 is never followed, because it is the path of greatest resistance.

In order to formulate the buckling problem, equation 5.17 can be rewritten in the form of:

$$\{K + \lambda K_g\} \{Q\} = \{R\} \tag{5.18}$$

{Q} is the transformed {U} vector needed to convert equation 5.17 into equation 5.18.

where K_σ is the geometric stiffness matrix for an arbitrary state of stress in the structure and λ is an orbitary scaler multiplier.

If the above system is in equilibrium, then addition of a virtual displacement pattern, {U} would keep the two configurations in equilibrium, (i.e.):

$$([K] + [K_\sigma]) \{U\} = \{R\} \tag{5.19a}$$

or

$$(K + \lambda[K_\sigma]) \{U\} = 0 \tag{5.19b}$$

Equation 5.19b has the form of a general eigenvalue problem where λ is equal to the load multiplier necessary to create buckling and {U} is buckling mode shape. It should be noted that the vector {U} is only a mode shape which gives the general pattern of displacement, and that the value of {U} at a certain point has no physical significance by itself. Also it is important to notice that the solution of equation 5.19b gives the overall buckling load of the structure as per this thesis requirements, and buckling of individual members cannot be predicted by this equation. A negative value for λ signifies that the overall structure is in tension and that the direction of all loads acting on the structure must be reversed to cause buckling.

5.3 GALERKIN FINITE ELEMENT FORMULATION OF THE HEAT CONDUCTION (GENERAL ENERGY) EQUATION:

The governing partial differential equation of heat conduction (general energy) in the cartesian coordinates is given by:

$$\frac{\partial}{\partial x}\left(K_x\frac{\partial\theta}{\partial x}\right) + \frac{\partial}{\partial y}\left(K_y\frac{\partial\theta}{\partial y}\right) + \frac{\partial}{\partial z}\left(k_z\frac{\partial\theta}{\partial z}\right) + Q_g - \rho C\frac{\partial\theta}{\partial t} \qquad (5.20)$$

The associated boundary conditions are:

1. Dirichlet boundary conditions (prescribed temperatures) $\theta = \theta^*$ on boundary S1. (5.21)

2. Neuman boundary conditions (prescribed heat flow)

$$-K_x\frac{\partial\theta}{\partial x}\eta_x - K_y\frac{\partial\theta}{\partial y}\eta_y - K_z\frac{\partial\theta}{\partial z}\eta_z + Q = 0 \qquad (5.22)$$

on boundary S2.

The Dirichlet boundary conditions in the present analysis are treated as a special case of Neuman boundary conditions by assuming a large value of convective heat transfer coefficient and an ambient temperature which is equal to the prescribed temperature.

Note that the value Q in the Neuman boundary conditions represents the total heat flux conducting into the body through the boundary on which Neuman boundary conditions are specified. For a simple case with no phase change condition, the conservation of heat flow at the boundary can be stated as:

Total heat flux input - Total heat flux conducting into the body

The total heat flux conducting into the body may be expressed as:

$$Q = Q_c + Q_r + Q_p \tag{5.23}$$

where

$$Q_c = \text{Total heat flux due to convection} = h_c(\theta_c - \theta) \tag{5.24}$$

$$Q_r = \text{Total heat flux due to radiation} = h_r(\theta_r - \theta) \tag{5.25}$$

where the equivalent radiation coefficient is given by:

$$h_r = \theta \epsilon \left(\theta_r^2 - \theta^2\right)(\theta_r + \theta)$$

$$Q^p = \text{Total prescribed heat flux} \tag{5.26}$$

5.3.1 GALERKIN FORMULATIONS:

Divide the domain into N finite elements. In each of these finite elements, assume the variation of temperature θ as a function of interpolations H_i and the nodal temperatures:

$$\theta(x,y,z,t) = [\, H(x,y,z)\,]\vec{\theta}^{(e)} = \sum H_j \theta_j \tag{5.27}$$

In Galerkin method, the integral of weighted residue over the domain is set to zero. The weights in this method are the same as the interpolation functions where $\iiint$ means $\oint_v$, a volume integral, and $\iint$ means $\int_\Gamma$, a surface integral.

$$\iiint H_i - \left\{\frac{\partial}{\partial x}\left(K_x\frac{\partial\theta}{\partial x}\right) + \frac{\partial}{\partial y}\left(K_y\frac{\partial\theta}{\partial y}\right) + \frac{\partial}{\partial z}\left(K_z\frac{\partial\theta}{\partial z}\right) + Q_g - \rho C\frac{\partial\theta}{\partial t}\right\} dx\,dy\,dz = 0 \tag{5.28}$$

Applying Green-Gauss (integrating by parts) theorem and using the equations (5.22 to 5.26), the equation (5.28) can be rewritten in the following form:

$$\iiint \left[\frac{\partial}{\partial x}H_i\cdot K_x\frac{\partial\theta}{\partial x} + \frac{\partial}{\partial y}H_i\cdot K_y\frac{\partial\theta}{\partial y} + \frac{\partial}{\partial z}H_i\cdot K_z\frac{\partial\theta}{\partial z}\right] dx\,dy\,dz \tag{5.29}$$

$$+ \iiint H_i\rho C\,\frac{\partial\theta}{\partial t}\,dx\,dy\,dz + \iint H_i\,(h_c + h_r)\theta\,ds$$

$$- \iiint H_i\theta_g\,dx\,dy\,dz + \iint h_i\,(h_c\theta_c + h_r\theta_r)\,ds + \iint H_i\theta_p\,ds$$

The above system of equations (for i = 1, N) can be expressed in matrix form as:

$$\left[\iiint\left\{\frac{\partial}{\partial x}[H]^T K_x \frac{\partial}{\partial x}[H] + \frac{\partial}{\partial y}[H]^T K_y \frac{\partial}{\partial y}[H] + \frac{\partial}{\partial z}[H]^T K_z \frac{\partial}{\partial z}[H]\right\} dx\,dy\,dz\right]\vec{\theta}$$

$$+ \left[\iint [H]^T (h_c + h_r)[H]\,ds\right]\vec{\theta} + \left[\iiint \rho\, C[H]^T[H]\,dx\,dy\,dz\right]\frac{\partial\vec{\theta}}{\partial t}$$

$$- \left[\iiint [H]^T Q_g\,dx\,dy\,dz\right] + \left[\iint [H]^T (h_c\theta_c + h_r\theta_r)\,ds\right] + \left[\iint [H]^T \theta_p\,ds\right] \qquad (5.30)$$

Thus the finite element system of equations can be rearranged in the following form:

$$\left[\,[K_k] + [K_c] + [K_r]\,\right]\vec{\theta} + [C]\,\dot{\vec{\theta}} = \vec{q}_g + \vec{q}_r + \vec{q}_c + \vec{q}_p$$

$$[K]\,\vec{\theta} + [C]\,\dot{\vec{\theta}} = \vec{q} \qquad (5.31)$$

Heat conduction matrix

$$[K_k] = \iiint [B]^T\,[K_T]\,[B]\,dx\,dy\,dz \qquad (5.32)$$

Thermal conductivity matrix

$$[K_T] = \begin{bmatrix} K_x & 0 & 0 \\ 0 & K_y & 0 \\ 0 & 0 & K_z \end{bmatrix} \qquad (5.33)$$

Thermal gradient matrix

$$[B] = \begin{bmatrix} \frac{\partial}{\partial x}[H] \\ \frac{\partial}{\partial y}[H] \\ \frac{\partial}{\partial z}[H] \end{bmatrix} \tag{5.34}$$

Heat convection matrix

$$[K_c] = \iint h_c [H]^T [H] \, ds \tag{5.35}$$

Heat radiation matrix

$$[K_r] = \iint h_r [H]^T [H] \, ds \tag{5.36}$$

Heat capacity matrix

$$[C] = \iiint \rho C [H]^T [H] \, dx dy dz \tag{5.37}$$

Thermal Load Vectors

Internal heat generation load vector

$$\vec{q}_g = \iiint [H]^T Q_g \, dx dy dz \tag{5.38}$$

Convective heat transfer load vector

$$\vec{q}_c = \iint h_c [H]^T \theta_c \, ds \tag{5.39}$$

Radiation heat transfer load vector

$$\vec{q}_r = \iint h_r [H]^T \theta_r \, ds \tag{5.40}$$

Prescribed heat flow load vector

$$\vec{q}_p = \iint [H]^T Q_p \, ds \tag{5.41}$$

5.3.2 SOLUTION PROCEDURES

5.3.2.1 LINEAR STEADY STATE ANALYSIS:

Since the temperature is not a function of time

$$\frac{\partial}{\partial t} (\vec{\theta}) = 0 \tag{5.42}$$

Equation (5.31) can be expressed as

$$[[K_k] + [K_c]] \vec{\theta} = \vec{q}_g + \vec{q}_c + \vec{q}_p \tag{5.43}$$

Note that the radiation boundary conditions are not present in the above equation because this is a linear analysis. Also note that the material properties and boundary conditions are not functions of either time or temperature.

Steady state nodal temperature distribution can be obtained by solving the above system of equations after applying the Dirichlet boundary conditions. The Dirichlet boundary conditions can be easily applied without disturbing the order of the matrices as follows:

Let the prescribed temperature of node "i" be θ^*. The two steps procedure is:

1. Replace the diagonal element of i^{th} row of effective conduction matrix [K] by a large number:

$$\text{i.e.,} \quad K_{ii} = 1.0E{+}15 \tag{5.44}$$

2. Replace the corresponding thermal load by the product of this large number and the prescribed temperature i.e.

$$q_i = (1.0E{+}15)\ \theta^* \tag{5.45}$$

Then solve the finite element system of equations to get the steady state temperature distribution.

5.3.2.2 LINEAR TRANSIENT ANALYSIS:

Analysis with constant material properties and constant boundary conditions with no radiation come under this category. Recalling the finite element system of equations:

$$[K]\,\vec{\theta} + [C]\,\dot{\vec{\theta}} = \vec{q} \tag{5.46}$$

Here $\dot{\theta}$ is the time derivative of the temperature. Assuming constant gradient in the neighborhood of time t, $\dot{\theta}$ may be expressed in any of the following methods:

Forward Difference Method

$$\dot{\vec{\theta}} = \left[{}^{(t+\Delta t)}\vec{\theta} - {}^{t}\vec{\theta} \right]/\Delta t \tag{5.47}$$

Backward Difference Method

$$\dot{\vec{\theta}} = \left[{}^{t}\vec{\theta} - {}^{(t-\Delta t)}\vec{\theta} \right]/\Delta t \tag{5.48}$$

Central Difference Method

$$\dot{\vec{\theta}} = \left[{}^{(t+\Delta t)}\vec{\theta} - {}^{(t-\Delta t)}\vec{\theta} \right] / \Delta t \tag{5.49}$$

In general, $\dot{\vec{\theta}}$ can be expressed as a function of a parameter α as follows:

$$t_{\dot{\vec{\theta}}} = \left[{}^{(t+\alpha\Delta t)}\vec{\theta} - {}^{t}\vec{\theta} \right] / (\alpha \Delta t) \tag{5.50}$$

since material properties are constant

$${}^{(t+\alpha\Delta t)}[K] = {}^{t}[K] \tag{5.51}$$

$${}^{(t+\alpha\Delta t)}[C] = {}^{t}[C] \tag{5.52}$$

Now consider the heat flow equilibrium at time, $t + \alpha\Delta t$,

$${}^{(t+\alpha\Delta t)}[K] \; {}^{(t+\alpha\Delta t)}\vec{\theta} + {}^{(t+\alpha\Delta t)}[C] \; {}^{(t+\alpha\Delta t)}\dot{\vec{\theta}} = {}^{(t+\alpha\Delta t)}\vec{q} \tag{5.53}$$

Substituting 5.50, 5.51, and 5.52 into 5.53 to get:

$$\left\{ [K] + \frac{1}{\alpha \Delta t} [C] \right\}^{(t+\alpha\Delta t)}\vec{\theta} = {}^{(t+\alpha\Delta t)}\vec{q} + \frac{1}{\alpha \Delta t} [C] \; {}^{t}\vec{\theta} \tag{5.54}$$

$$[K^*]\,{}^{(t+\alpha\Delta t)}\vec{\theta} = {}^{(t+\alpha\Delta t)}\vec{q} + {}^{t}\vec{E} \tag{5.55}$$

With the known load vector at time, t + αΔt, the temperature distribution at time, t + αΔt, can be obtained by solving the equation 5.55.

Then the temperature distribution at time, t + Δt, can be obtained as:

$${}^{(t+\Delta t)}\vec{\theta} = \left(1 - \frac{1}{\alpha}\right){}^{t}\vec{\theta} + \frac{1}{\alpha}\,{}^{(t+\alpha\Delta t)}\vec{\theta} \tag{5.56}$$

Note that matrix [K*] is independent of the temperature distribution, i.e. [K*] is constant throughout the solution. Hence, the triangularization of the matrix [K*] is to be done only once for the entire solution process.

At each time step, the load vector corresponding to the time, t + αΔt, and the temperature distribution at same time step, t + αΔt, can be obtained by back substitution. Then the temperature at time, t + Δt, can be obtained using equation 5.56. A step by step procedure to solve linear transient heat conduction problems is:

Initial calculations

1. Form heat conduction matrix $[K_k]$

2. Form heat convection matrix [K_c] (if required)

3. Form heat capacity matrix [C]

4. Compute the effective conduction matrix as:

$$[K^*] = [K_k] + [K_c] + \frac{1}{\alpha \Delta t}[C]$$

5. Modify [K^*] for temperature boundary conditions

6. Compute the initial resistance vector

$$\vec{E}_0 = \frac{1}{\alpha \Delta t}[C]\,\vec{\theta}_0$$

7. Triangularize effective conduction matrix [K^*]

<u>For each solution time step, follow the solution below:</u>

1. Form the heat flow vector ${}^{(t+\alpha\Delta t)}\vec{q}$ at time, t + $\alpha\Delta$t

2. Compute the resistance vector

$${}^{t}\vec{E} = \frac{1}{\alpha \Delta t}[C]\,{}^{t}\vec{\theta}$$

3. Compute the effective heat flow vector

$${}^{(t+\alpha\Delta t)}\vec{Q} = {}^{(t+\alpha\Delta t)}\vec{q} + {}^{t}\vec{E}$$

4. Modify load vector for temperature boundary conditions

5. Solve the heat flow equilibrium equations for the temporature distribution at time, t + $\alpha\Delta t$:

$$[K^*]\,{}^{(t+\alpha\Delta t)}\vec{\theta} = {}^{(t+\alpha\Delta t)}\vec{q}$$

6. Compute the temperature distribution at time, t + Δt, as:

$${}^{(t+\Delta t)}\vec{\theta} = \left(1 - \frac{1}{\alpha}\right)^{t}\vec{\theta} + \frac{1}{\alpha}\,{}^{(t+\alpha\Delta t)}\vec{\theta}$$

7. Return back and proceed to step 1 to find the temperature distribution for the next time step. Otherwise, stop the solution procedure according to convergence criteria or procedure ending concept.

5.3.2.3 NON-LINEAR TRANSIENT ANALYSIS:

Recall the governing system of the finite element equations:

$$\left[\,[K_k] + [K_c] + [K_r]\,\right]\vec{\theta} + [C]\dot{\vec{\theta}} = \vec{q}_g + \vec{q}_c + \vec{q}_r + \vec{q}_p \qquad (5.57)$$

Rearrange the above system of equations in the following form:

Rearrange the above system of equations in the following form:

$$[K]\vec{\theta} + [C]\dot{\vec{\theta}} = \vec{q} \tag{5.58}$$

where the equivalent conduction matrix is:

$$[K] = [K_k] + [K_c] + [K_r] \tag{5.59}$$

and the equivalent thermal load vector is:

$$\vec{q} = \vec{q}_g + \vec{q}_c + \vec{q}_r + \vec{q}_p \tag{5.60}$$

It is obvious that the temperature dependent material properties and the radiation boundary conditions make this system of equations highly non-linear. Hence, it is appropriate to use incremental solution procedure, i.e. calculation of temperature distribution at time, $t+\alpha\Delta t$, from the known temperature distribution at time, t. Hence, consider the heat flow equilibrium at time, $t+\alpha\Delta t$:

$$^{(t+\alpha\Delta t)}[K]\ ^{(t+\alpha\Delta t)}\vec{\theta} + {}^{(t+\alpha\Delta t)}[C]\ ^{(t+\alpha\Delta t)}\dot{\vec{\theta}} = {}^{(t+\alpha\Delta t)}\vec{q} \tag{5.61}$$

where the left superscript denotes the time.

Since the matrices [K] and [C] are functions of temperature, the solution process can be started with the following linearization:

$$^{(t+\alpha\Delta t)}[K] \approx {}^{t}[K] \tag{5.62}$$

$$^{(t+\alpha\Delta t)}[C] \approx {}^{t}[C] \tag{5.63}$$

$$^{(t+\alpha\Delta t)}\vec{\theta} \approx {}^{t}\vec{\theta} + \overline{\Delta\theta}^{(0)} \tag{5.64}$$

where $\overline{\Delta\theta}^{(0)}$ is a vector of incremental temperatures between times t and t+$\alpha\Delta$t. The linearized system of equations can be represented as:

$$^{t}[K]\ ^{(t+\alpha\Delta t)}\vec{\theta} + {}^{t}[C]\ ^{(t+\alpha\Delta t)}\dot{\vec{\theta}} = {}^{(t+\alpha\Delta t)}\vec{q} \tag{5.65}$$

Assuming linear variation of temperature over the time increment:

$$\dot{\vec{\theta}} = \left[\frac{^{(t+\alpha\Delta t)}\vec{\theta} - {}^{t}\vec{\theta}}{\alpha\Delta t}\right] \tag{5.66}$$

Substitute 5.66 into 5.65 and rearrange terms to get:

$$\left[{}^{t}[K] + \frac{1}{\alpha\Delta t}\,{}^{t}[C]\right]\overline{\Delta\theta}^{(0)} = {}^{(t+\alpha\Delta t)}\vec{q} - {}^{t}[K]\ {}^{t}\vec{\theta} \tag{5.67}$$

solution of this system of equations gives the first approximation of incremental temperatures. Hence, the approximate temperatures at time, $t + \alpha\Delta t$, are given by:

$$^{(t+\alpha\Delta t)}\vec{\theta} = {}^{t}\vec{\theta} + \overline{\Delta\vec{\theta}}^{(0)} \tag{5.68}$$

Therefore, the temperatures at time, $t + \Delta t$, are computed as:

$$^{(t+\Delta t)}\vec{\theta}^{(0)} = \frac{1}{\alpha}\,{}^{(t+\alpha\Delta t)}\vec{\theta}^{(0)} + \left(1 - \frac{1}{\alpha}\right){}^{t}\vec{\theta} \tag{5.69}$$

5.3.2.4 EQUILIBRIUM ITERATIONS TO APPROACH THE CORRECT SOLUTION (CONVERGENCE):

Solution of the equation 5.67 does not give the correct incremental temperatures because of the linearization of equation 5.61, i.e. the substitution of this solution into equation 5.61 gives an unbalanced heat flow. Hence, this solution has to be updated to take care of this unbalanced heat flow. This procedure should be repeated until the residual heat flow is within the required tolerance. These iterations which achieve the heat flow equilibrium are called equilibrium iterations.

The temperature correction at the end of iteration "i" may be expressed as:

$$ {}^{(t+\alpha\Delta t)}\vec{\theta}^{(i)} = {}^{(t+\alpha\Delta t)}\vec{\theta}^{(i-1)} + \overrightarrow{\Delta\Delta\theta}^{(i)} \tag{5.70} $$

and

$$ \overrightarrow{\Delta\Delta\theta}^{(i)} = \overrightarrow{\Delta\theta}^{(i)} - \overrightarrow{\Delta\theta}^{(i-1)} \tag{5.71} $$

where $\overrightarrow{\Delta\Delta\theta}^{(i)}$ is the correction in incremental temperatures during iteration "i." Now, consider the heat flow equilibrium of equation 5.61 at the end of iteration "i":

$$ {}^{(t+\alpha\Delta t)}[K]\ {}^{(t+\alpha\Delta t)}\vec{\theta}^{(i)} + {}^{(t+\alpha\Delta t)}[C]\left\{\frac{{}^{(t+\alpha\Delta t)}\vec{\theta}^{(i)} - {}^{t}\vec{\theta}}{\alpha\Delta t}\right\} = {}^{(t+\alpha\Delta t)}\vec{q} \tag{5.72} $$

Substitute equation 5.70 into 5.72 to get:

$$ \left[{}^{(t+\alpha\Delta t)}[K] + \frac{1}{\alpha\Delta t}\,{}^{(t+\alpha\Delta t)}[C]\right]\overrightarrow{\Delta\Delta\theta}^{(i)} $$

$$ = {}^{(t+\alpha\Delta t)}\vec{q} - {}^{(t+\alpha\Delta t)}[K]\ {}^{(t+\alpha\Delta t)}\vec{\theta}^{(i-1)} - {}^{(t+\alpha\Delta t)}[C]\ {}^{(t+\alpha\Delta t)}\dot{\vec{\theta}}^{(i-1)} \tag{5.73} $$

Corrections for incremental temperatures may be obtained by solving the equation 5.73. On close observation, it is obvious that this method is similar to the Newton-Raphson solution of equation 5.61. Note that this method requires the triangularization of the coefficients matrix in each

iteration which is very expensive. Hence, a modified Newton-Raphson scheme is followed in which the coefficients matrix is not updated in each iteration. Thus each iteration only involves a back substitution which is very inexpensive.

The governing equations for the modified Newton-Raphson iterations are:

$$\left[{}^{t}[K] + \frac{1}{\alpha \Delta t} {}^{t}[C] \right] \overrightarrow{\Delta\Delta\theta}^{(i)}$$

$$= {}^{(t+\alpha\Delta t)}\vec{q} - {}^{(t+\alpha\Delta t)}[K]\, {}^{(t+\alpha\Delta t)}\vec{\theta}^{(i-1)} - {}^{(t+\alpha\Delta t)}[C]\, {}^{(t+\alpha\Delta t)}\dot{\vec{\theta}}^{(i-1)} \tag{5.74}$$

$$\overrightarrow{\Delta\theta}^{(i)} = \overrightarrow{\Delta\theta}^{(i-1)} + \overrightarrow{\Delta\Delta\theta}^{(i)} \tag{5.75}$$

$${}^{(t+\alpha\Delta t)}\vec{\theta}^{(i)} = {}^{(t+\alpha\Delta t)}\vec{\theta}^{(i-1)} + \overrightarrow{\Delta\Delta\theta}^{(i)} \tag{5.76}$$

Repeat the above calculations until convergence is achieved.

5.3.2.5 CONVERGENCE CRITERIA:

It is assumed that the solution has converged if the following criteria is satisfied:

$$\frac{\| \overrightarrow{\Delta\Delta}\theta^{(i)} \|_2}{\| {}^{(t+\alpha\Delta t)}\vec{\theta}^{(i)} \|_2} < \text{Convergence tolerance} \qquad (5.77)$$

where the Convergence tolerence is 0.00001 for this thesis, and the norm of vector V is:

$$\| V \|_2 = \sqrt{V_1^2 + V_2^2 + V_3^2 + \ldots + V_n^2} \qquad (5.78)$$

$V_1, V_2, \ldots V_n$ being the components of the Vector V. The temperature distribution at time, $t + \Delta t$, may be obtained from the temperature distribution at time, $t + \alpha\Delta t$, from the equation:

$${}^{(t+\Delta t)}\vec{\theta} = \frac{1}{\alpha} {}^{(t+\alpha\Delta t)}\vec{\theta}^{(i)} + \left(1 - \frac{1}{\alpha}\right) {}^{t}\vec{\theta} \qquad (5.79)$$

Repeat this procedure to find the temperature distribution at all other required time steps. A step by step procedure to solve the non-linear transient heat conduction problems is as follows:

Initial calculations

1. Define initial temperature vector

2. Initialize time step counter

3. Form conduction matrix [K_k]

4. Form convection matrix [K_c] (if required)

5. Form radiation matrix [K_r] (if required)

6. Form heat capacity matrix [C]

7. Compute the effective conduction matrix:

$$[K^*] = [K_k] + [K_c] + [K_r] + \frac{1}{\alpha \Delta t}[C]$$

8. Modify [K^*] for temperature boundary conditions

9. Compute the initial heat flow vector due to conduction

$$\vec{F}_0 = \left[{}^t[K_k] + {}^t[K_c] + {}^t[K_r] \right] {}^t\vec{\theta}$$

10. Triangularize the matrix [K^*]

For each solution time step, follow the solution procedure given below:

1. Increment the time step counter

KSTEP = KSTEP + 1

2. Increment the time

   TIME = TIME + $\alpha\Delta t$

   where Δt is the time step increment. In case of variable time step analysis, substitute the appropriate time step increment in the above equation.

3. Check for matrix reformation?

   NO: Advance to step 9

   IF (KSTEP.EQ.1) advance to step 9

   YES: Continue

4. Form heat conduction, convection, radiation and heat capacity matrices corresponding to the temperature distribution at the end of the last time step.

5. Compute the effective conduction matrix as:

$$[K^*] = [K_k] + [K_c] + [K_r] + \frac{1}{\alpha \Delta t}[C]$$

6. Modify [K*] for temperature boundary conditions

7. Compute the internal flow vector due to conduction

$$^{t}\vec{F} = \left\{ {}^{t}[K_k] + {}^{t}[K_c] + {}^{t}[K_r] \right\} {}^{t}\vec{\theta}$$

8. Triangularize matrix $[K^*]$

9. Define the heat flow vector at time, $t + \alpha\Delta t$, i.e. ($^{(t+\alpha\Delta t)}\vec{q}$)

10. Compute the effective heat flow vector

$$^{(t+\alpha\Delta t)}\vec{q}^{*} = {}^{(t+\alpha\Delta t)}\vec{q} - {}^{t}\vec{F}$$

11. Solve the following system of equations for nodal temperature increments $\overline{\Delta\theta}^{(0)}$ by back substitution

$$[K^*]\overline{\Delta\theta}^{(0)} = {}^{(t+\alpha\Delta t)}\vec{q}^{*}$$

12. Check for heat flow equilibrium?

    YES: Advance to step 16

    NO: Continue

13. Find the temperature distribution at time, $t + \alpha\Delta t$

$$^{(t+\alpha\Delta t)}\vec{\theta} = {}^{t}\vec{\theta} + \overline{\Delta\theta}^{(0)}$$

14. Find the temperature distribution at time, $t + \Delta t$

$$^{(t+\Delta t)}\vec{\theta} = \frac{1}{\alpha}\,^{(t+\alpha\Delta t)}\vec{\theta} + \left(1 - \frac{1}{\alpha}\right)\,^{t}\vec{\theta}$$

15. Check for the total number of solution time steps.

    IF (KSTEP.LT.NSTEP) Go to step 1

    Otherwise, stop the solution

16. Initialize iteration counter I = 0

17. Compute the temperature distribution at the beginning of the first equilibrium iteration

$$^{(t+\alpha\Delta t)}\vec{\theta}^{(0)} = {}^{t}\vec{\theta} + \overline{\Delta\theta}^{(0)}$$

18. Increment the iteration counter

    I = I + 1

19. Compute the nodal temperatures and the time derivatives at the end of the previous iteration

$$^{(t+\alpha\Delta t)}\vec{\theta}^{(I-1)} = {}^{t}\vec{\theta} + \overline{\Delta\theta}^{(I-1)}$$

$$^{(t+\alpha\Delta t)}\dot{\vec{\theta}}^{(I-1)} = \left[\frac{^{(t+\alpha\Delta t)}\vec{\theta}^{(I-1)} - {}^{t}\vec{\theta}}{\alpha\Delta t}\right]$$

20. Calculate the out of balance heat flow vector

$$\vec{q}_{bal} = {}^{(t+\alpha\Delta t)}[K]\,{}^{(t+\alpha\Delta t)}\vec{\theta}^{(i-1)} + {}^{(t+\alpha\Delta t)}[C]\,{}^{(t+\alpha\Delta t)}\dot{\vec{\theta}}^{(i-1)}$$

21. Compute the effective heat flow vector

$${}^{(t+\alpha\Delta t)}\vec{q}^{*} = {}^{(t+\alpha\Delta t)}\vec{q} - \vec{q}_{bal}$$

22. Solve for the corrections in temperature increments by back substitution

$$[K^{*}]\overrightarrow{\Delta\Delta\theta}^{(i)} = {}^{(t+\alpha\Delta t)}\vec{q}^{*}$$

23. Compute the total increments in temperature and temperature at time, $t + \alpha\Delta t$

$$\overrightarrow{\Delta\theta}^{(i)} = \overrightarrow{\Delta\theta}^{(i-1)} + \overrightarrow{\Delta\Delta\theta}^{(i)}$$

$${}^{(t+\alpha\Delta t)}\vec{\theta}^{(i)} = {}^{(t+\alpha\Delta t)}\vec{\theta}^{(i-1)} + \overrightarrow{\Delta\Delta\theta}^{(i)}$$

24. Check for convergence

$$\frac{\| \overrightarrow{\Delta\Delta\theta}^{(i)} \|_2}{\| {}^{(t+\alpha\Delta t)}\vec{\theta}^{(i)} \|_2} < \text{Convergence tolerance}$$

If convergence: advance to step 25

IF (I .LT. Max. no. of iterations) go to step 18

Otherwise, restart using smaller time step or increase the maximum allowable number of iterations

25. Compute the temperature distribution at the end of time, t + Δt

$$^{(t+\Delta t)}\vec{\theta} = \frac{1}{\alpha}\,{}^{(t+\alpha\Delta t)}\vec{\theta}^{(i)} + \left(1 - \frac{1}{\alpha}\right)\,{}^{t}\vec{\theta}$$

26. Check for the total number of solution time steps?

IF (KSTEP.LT.NSTEP) go to step 1

Otherwise, stop the solution.

CHAPTER 6

ANALYSIS AND RESULTS

This is the chapter of analysis and results. Here, all the relevant input and output data are displayed for both the stress buckling loads and the heat transfer analysis together with the subsequent thermal stress analysis. Color presentations of stress and thermal modes, contours, and other parameters are shown. They are indicative, successful, accurate and perhaps impressive.

Enclosed are the relevant input and output data from the input and output files of some of the problems run by the COSMOS/M program. A total of thirteen drawings are displayed. The program uses shell of revolution elements to solve the buckling problems subjected to symmetric and asymmetric static and dynamic loads. Significant amounts of engineering time are saved by using shell of revolution elements rather than general shell elements. The external load is decomposed into Fourier components and the

stress solution is composed of these Fourier components or a summation of them. Buckling is solved in terms of Fourier components.

The geometric modeler part defines the key points and boundaries to create the problem 3-D mesh interactively. The advance dynamic analysis performs a step by step time history analysis, frequency response, mode shapes, and buckling response. Heat transfer analysis is fully done for the transient state.

BUCKLING:

The Figures 6.1, 6.2, and 6.3 show buckling loads and modes of the laminated composite panel as had been described in the original drawings. As mentioned before, only a quarter of the panel was considered (upper right section) due to symmetry. Two types of boundary conditions, namely simply supported and fixed, were accounted for. The buckling loads indicated for each case are in terms of pounds per unit length (lbs/in). For the (simply-supported) boundry conditions all four edges were considered as such, with three edges of the panel being free to move in the x-direction. All four edges were considered fixed for the (fixed-fixed) boundry conditions except for motion in the x-direction along three edges.

THERMAL:

The heat transfer analysis was performed by applying the specified heat flux on the circular region in the middle of the panel in accordance with the time curve specified by the NRL. The thermal output results were displayed graphically for several different time steps. Figures 6.4 through 6.7 show the temperature distribution for time steps 1, 10, 12, and 25 respectively.

Subsequently a thermal stress analysis was performed by applying the temperature distribution acquired from the heat transfer analysis. Figures 6.8 through 6.13 show the stress distribution for temperatures of time steps 1 and 25. Three components of stress are considered for each case.

INPUT AND OUTPUT FILES (DATA AND RESULTS):

1. BUCK1SES: An input file giving in the data for the simply supported boundary conditions of the laminated composite panel in static buckling.

2. BUCK2SES: An input file giving in the data for the encastré (fixed-fixed) boundary conditions of the laminated composite panel in static buckling.

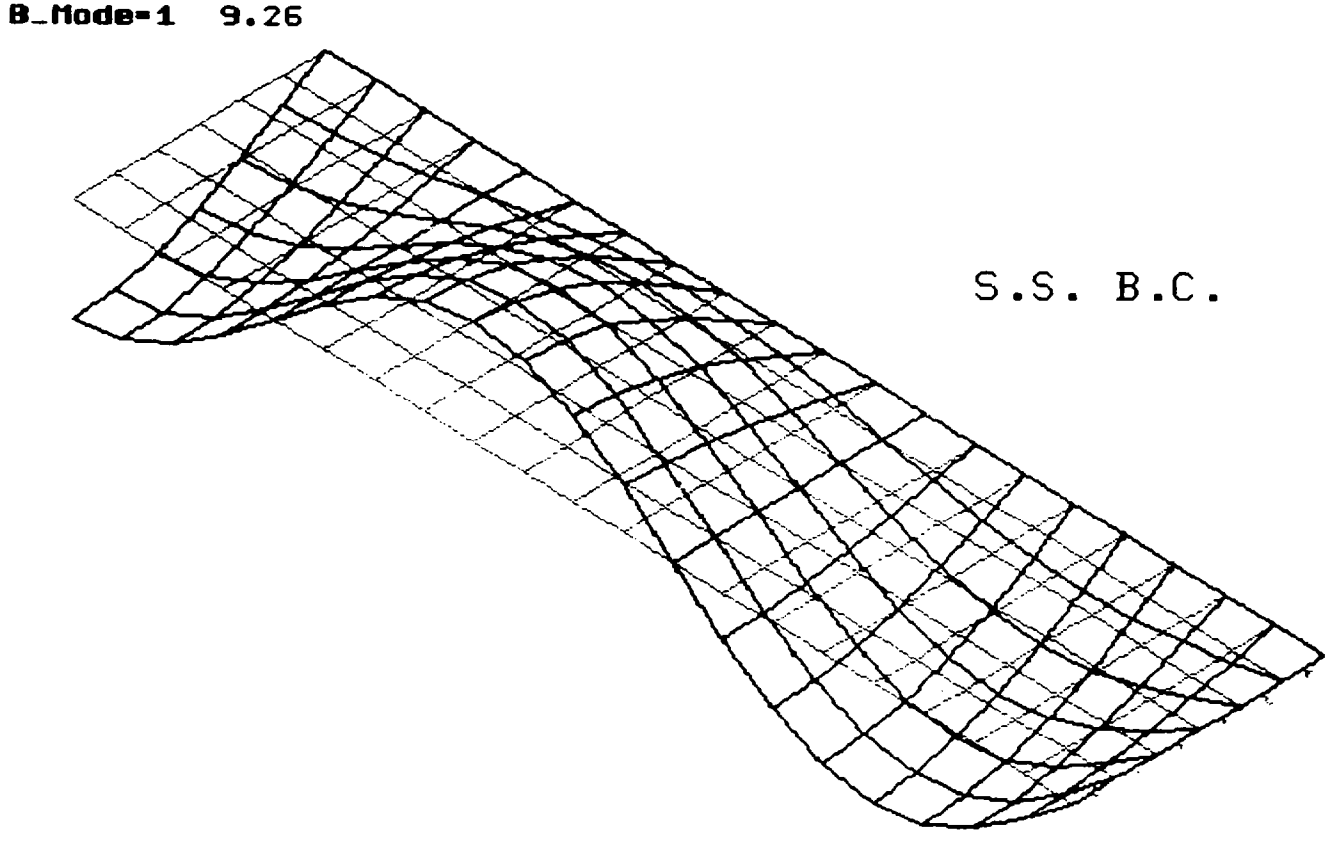

Figure 6.1
Simply-Supported Boundary
Condition for Buckling Mode 1

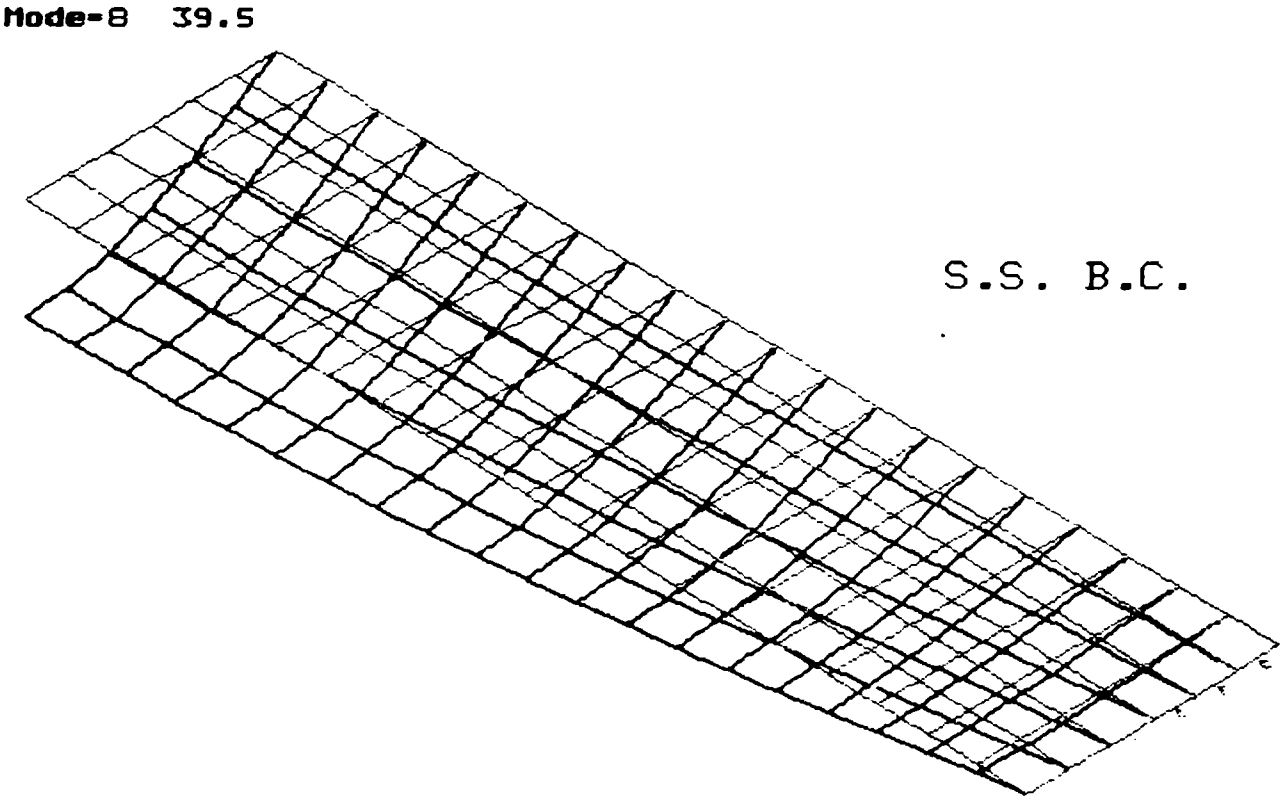

Figure 6.2
Simply-Supported Boundary
Condition for Buckling Mode 8

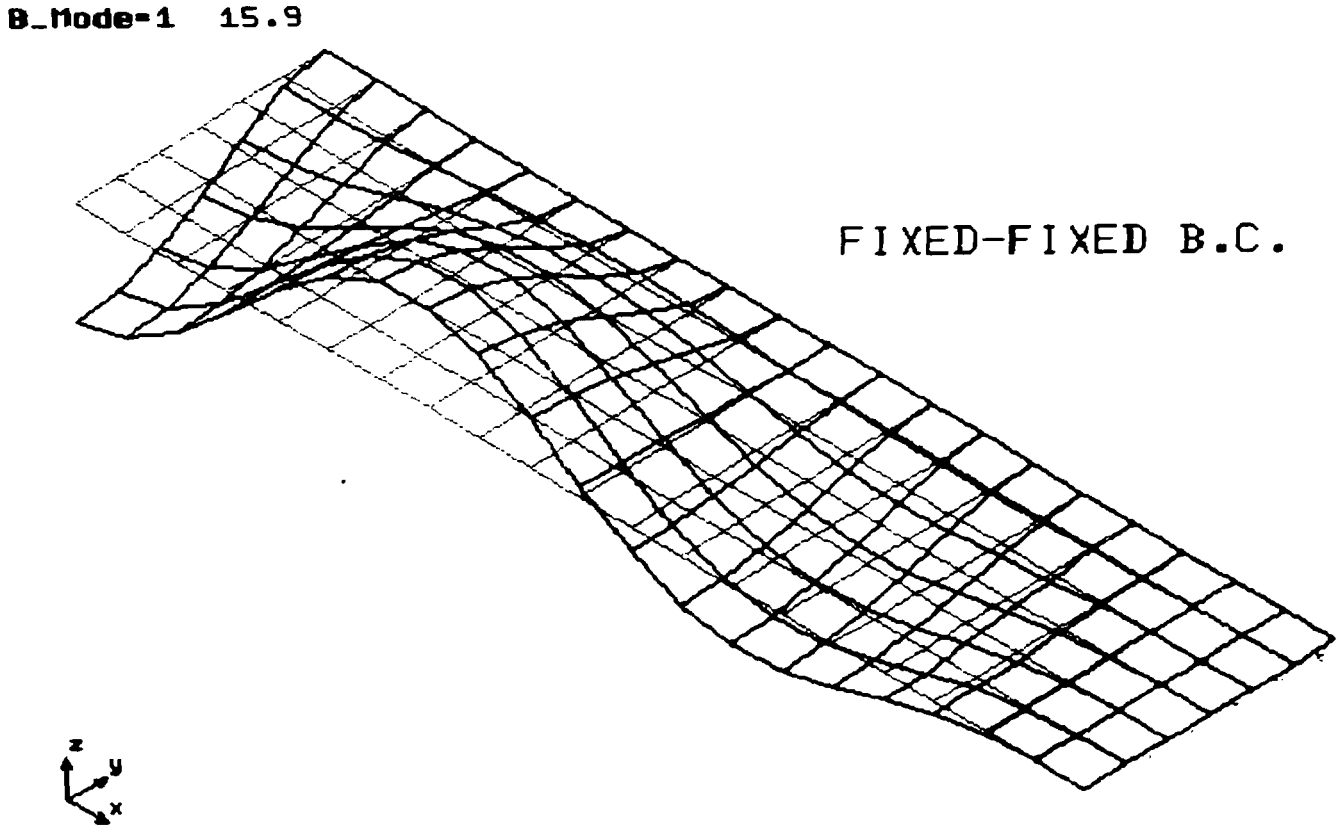

Figure 6.3
Fixed-Fixed Boundary Condition
for Buckling Mode 1

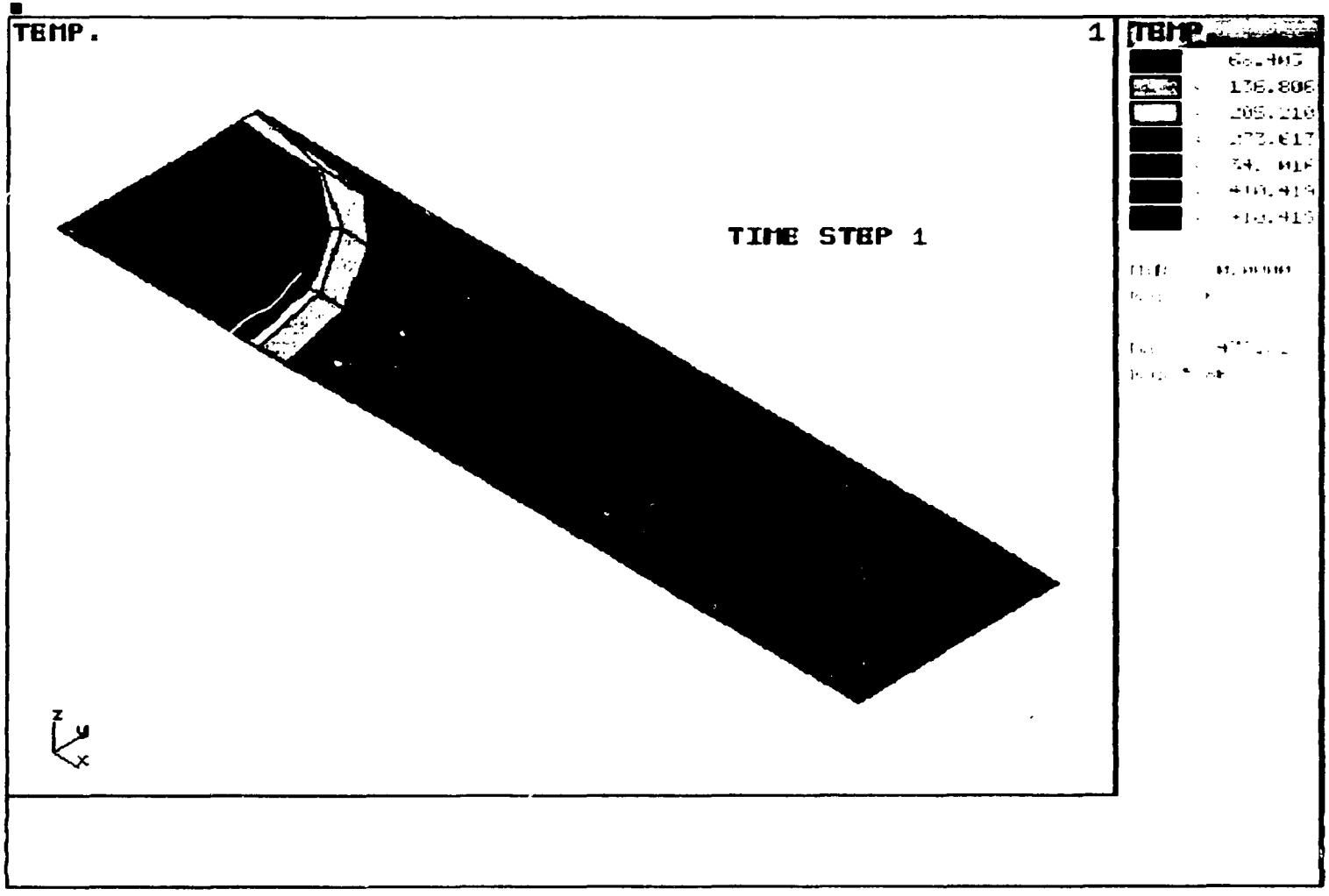

Figure 6.4
Temperature Distribution -
Time Step 1

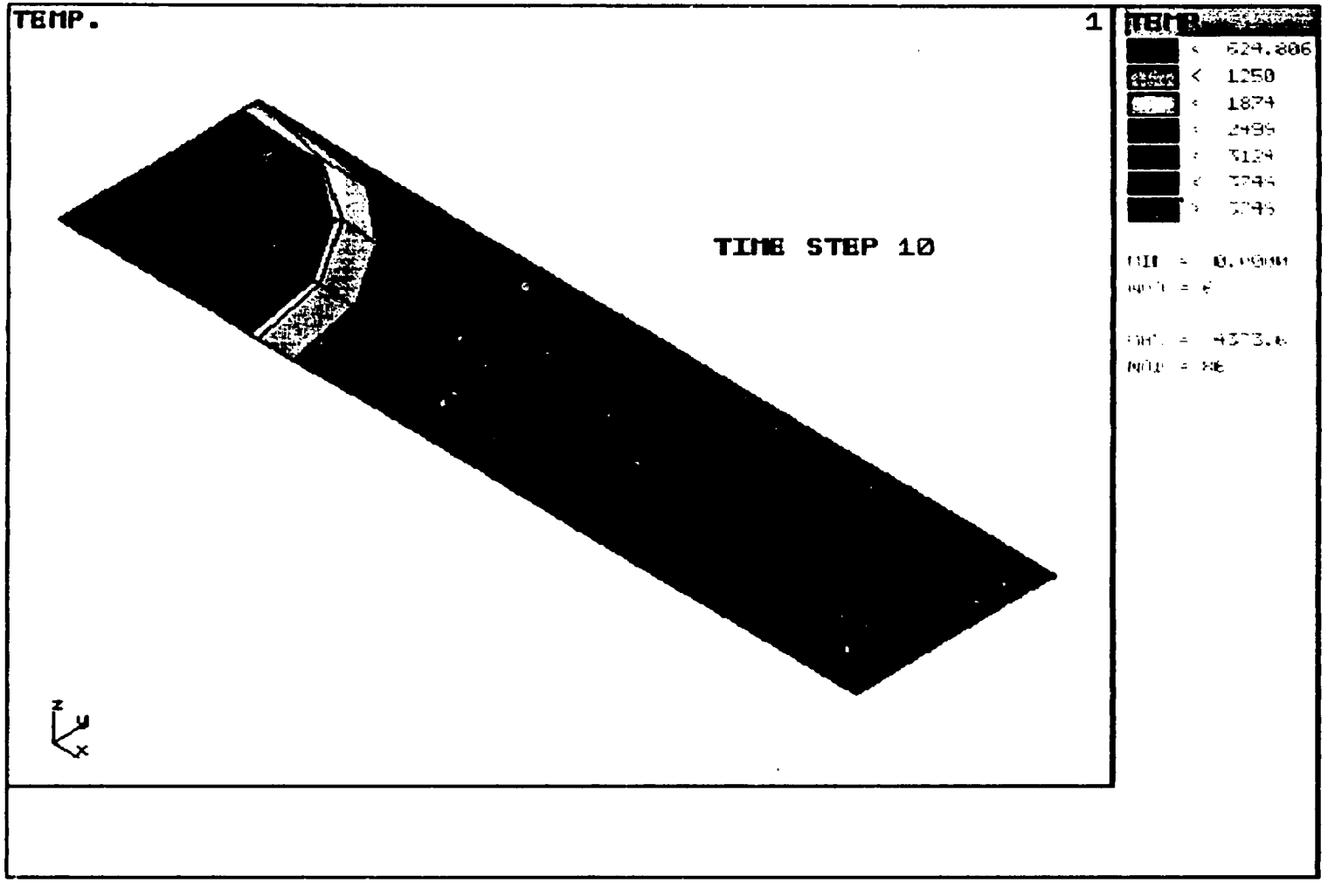

Figure 6.5
Temperature Distribution -
Time Step 10

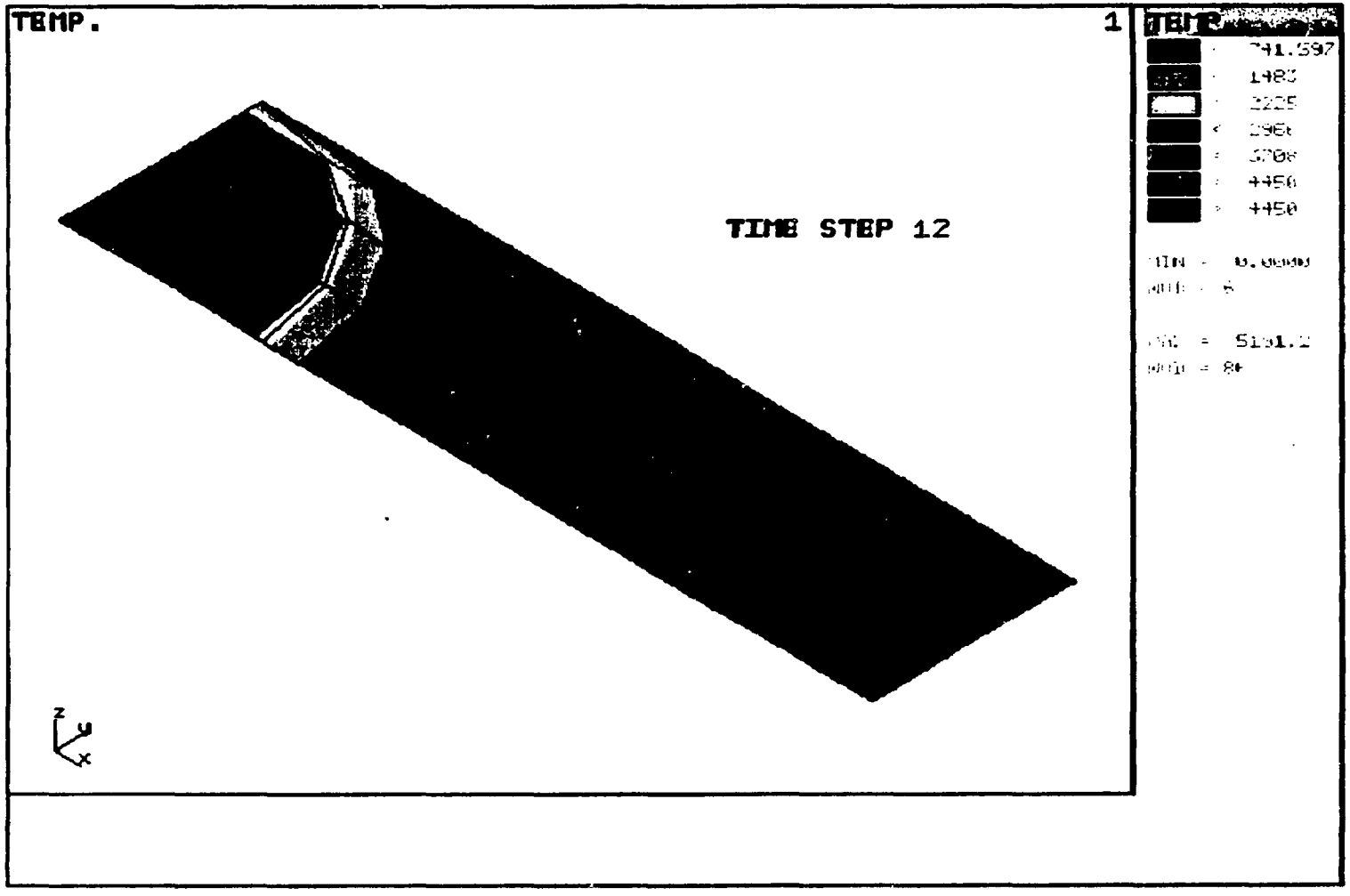

Figure 6.6
Temperature Distribution -
Time Step 12

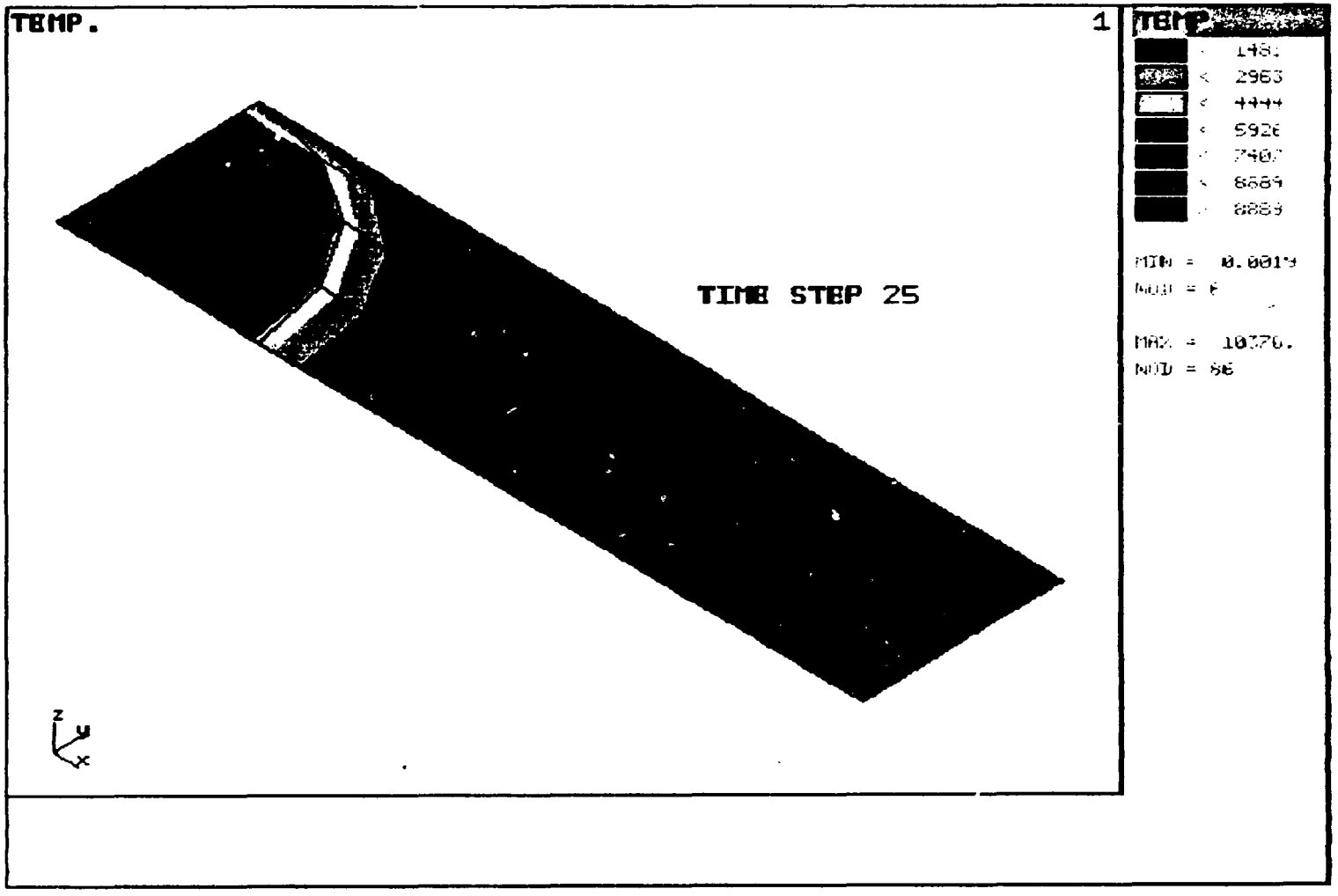

Figure 6.7
Temperature Distribution -
Time Step 25

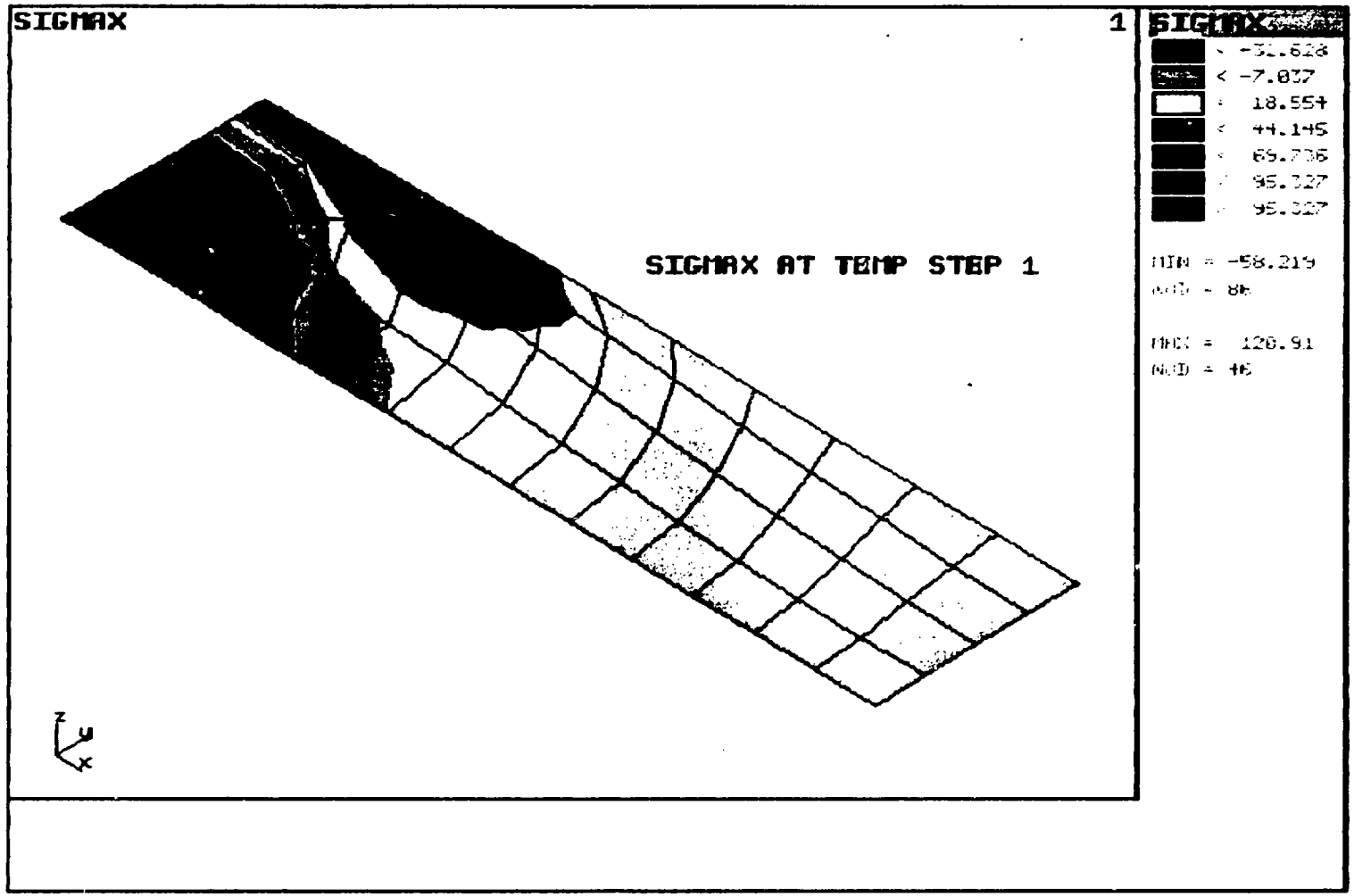

Figure 6.8
Stress in X Direction -
Time Step 1

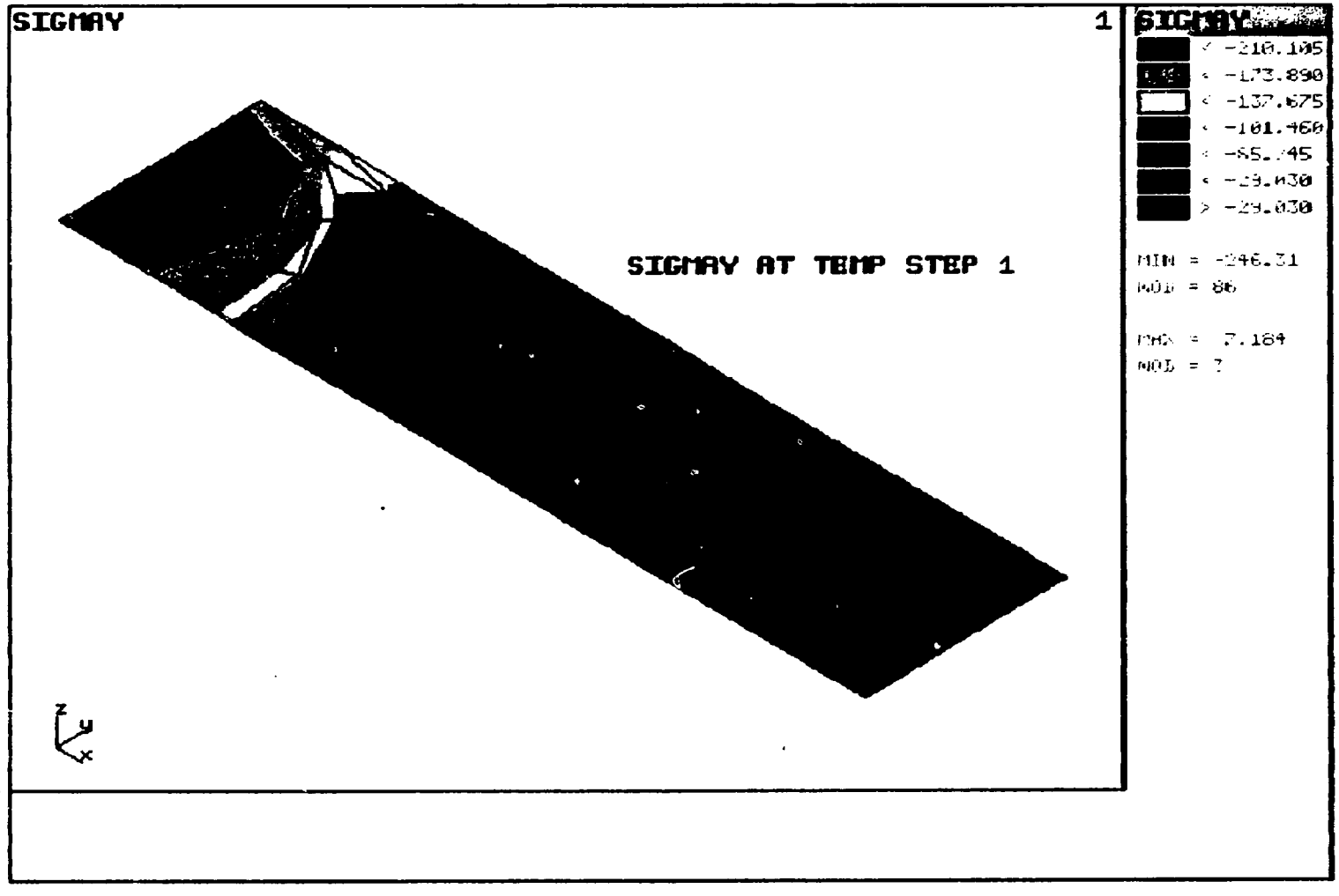

Figure 6.9
Stress in Y Direction -
Time Step 1

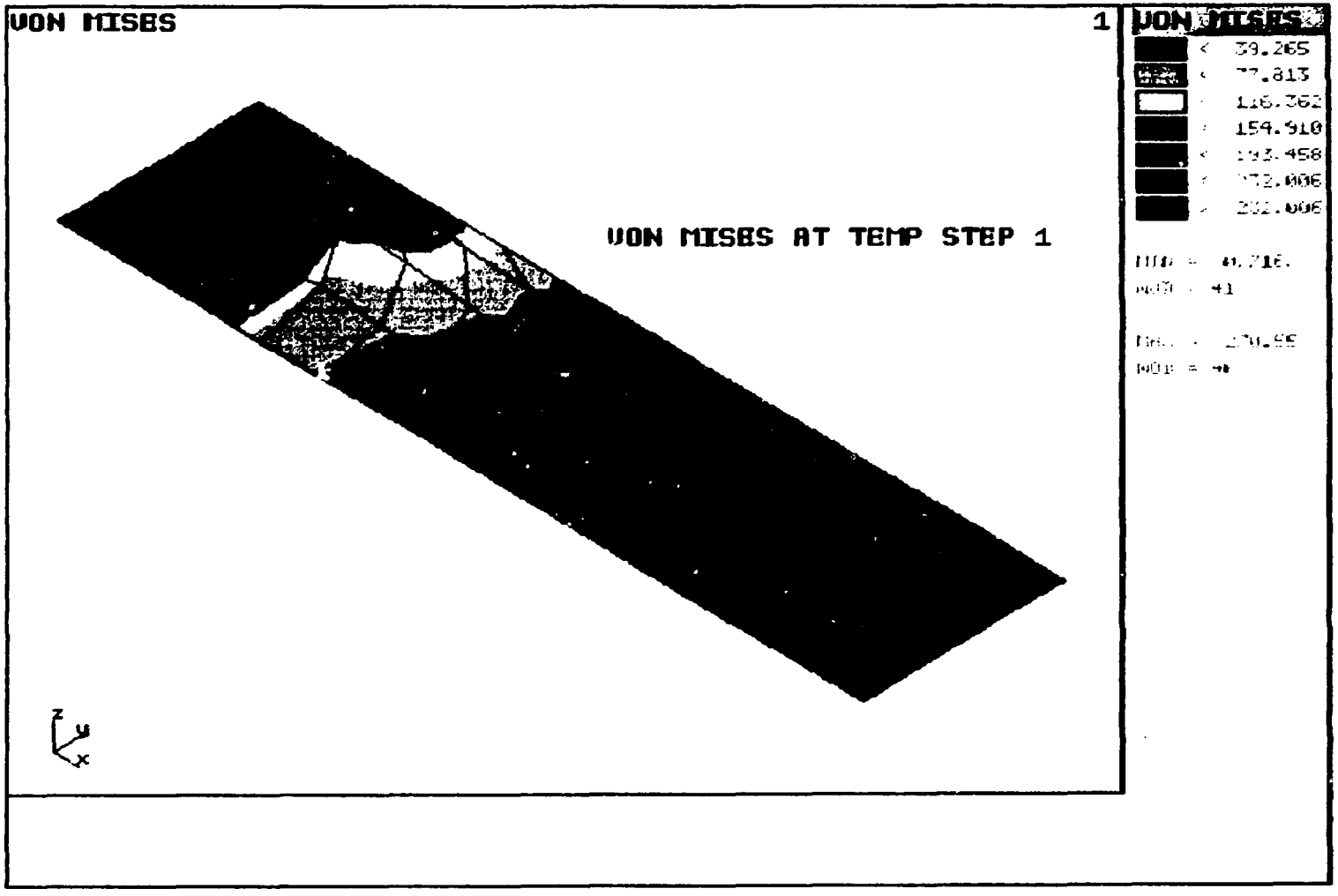

Figure 6.10
Von Mises - Time Step 1

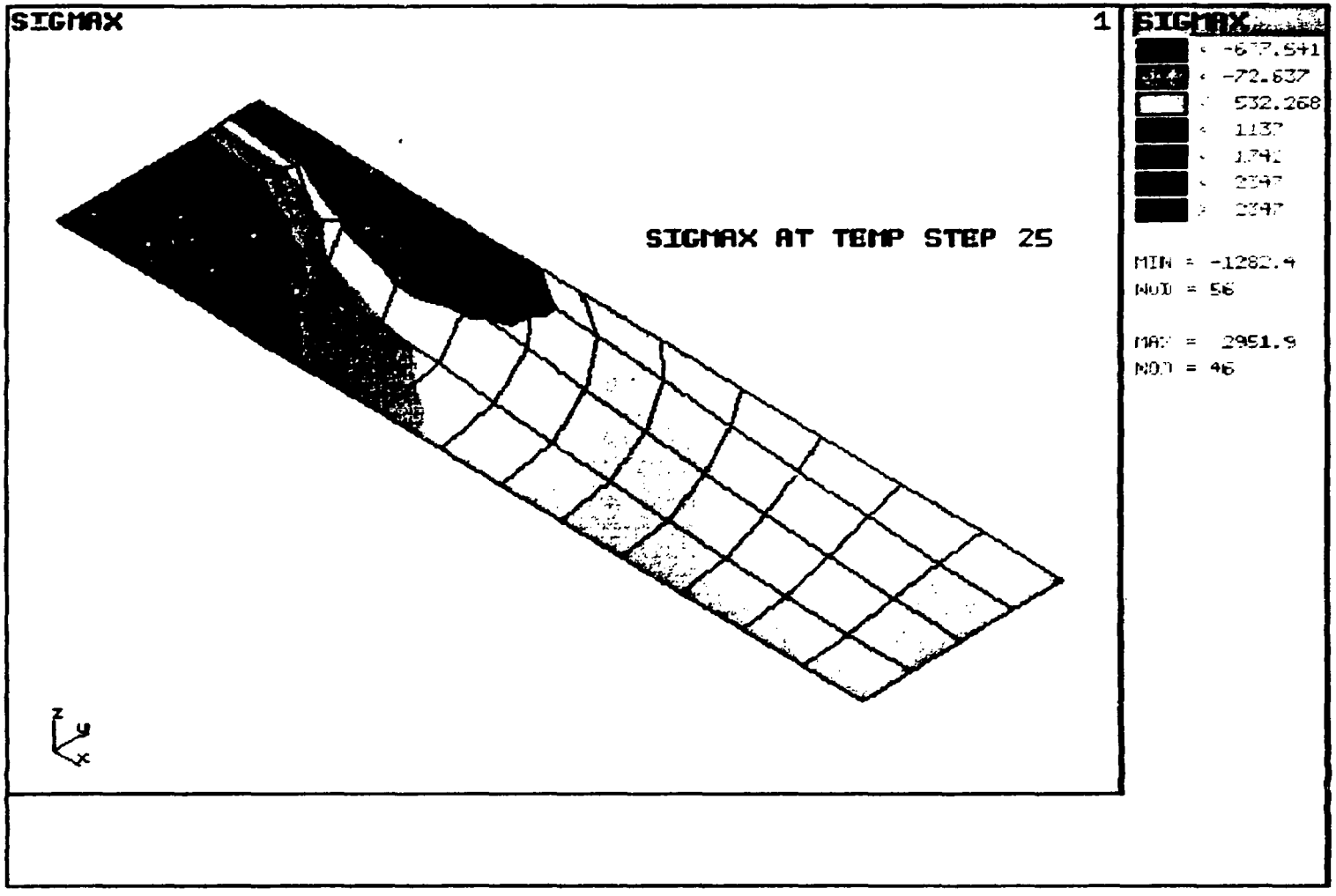

Figure 6.11
Stress in X Direction -
Time Step 25

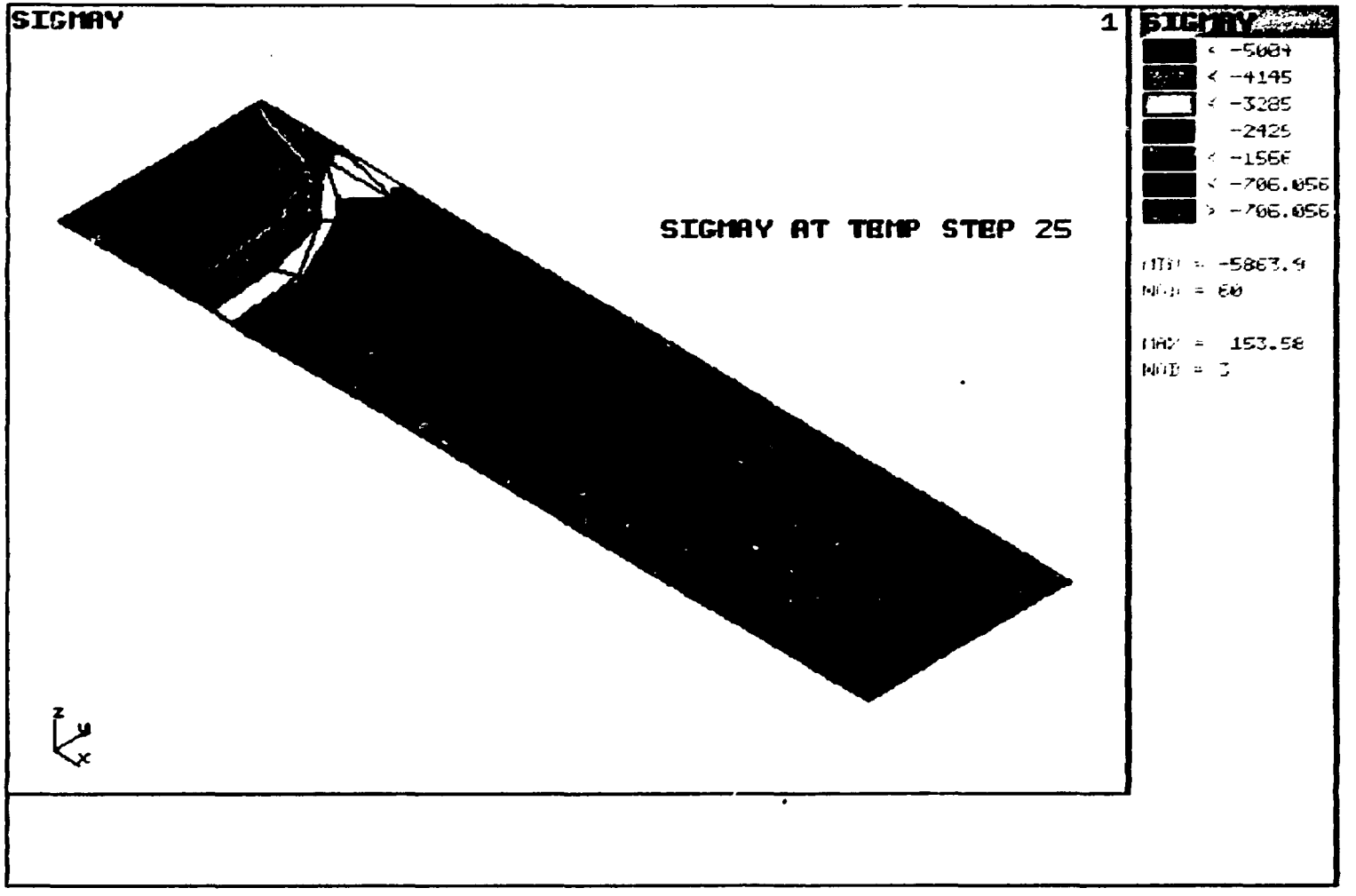

Figure 6.12
Stress in Y Direction -
Time Step 25

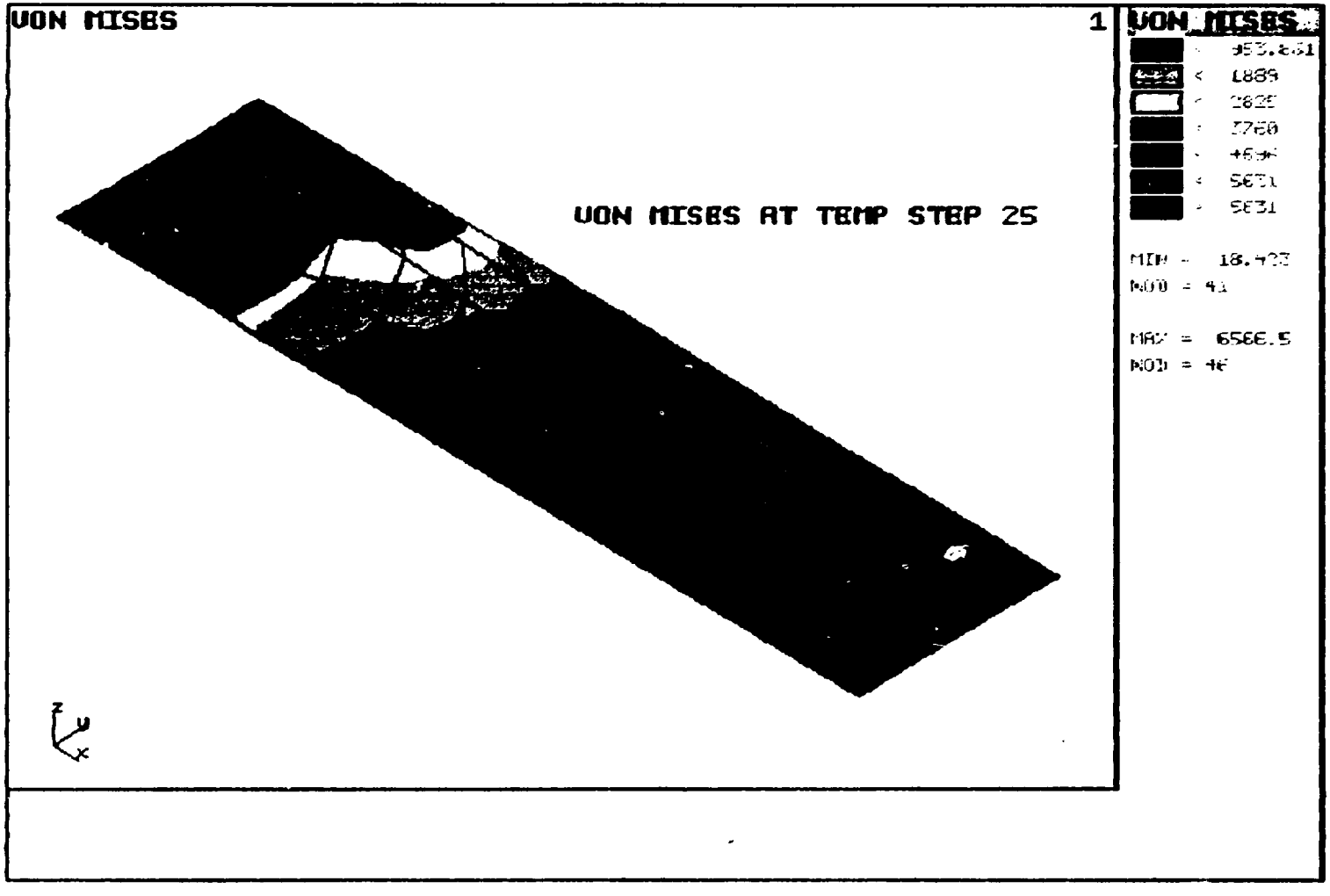

Figure 6.13
Von Mises - Time Step 25

3. T1.LOG: An input file giving in the material properties and specified temperature and flux boundary conditions to go from heat transfer to stress. Such properties included Young's Modulus of Elasticity in each cartesian coordinate direction, Poisson's ratio in each cartesian coordinate direction, thermal conductivity in each cartesian coordinate direction, specific heat capacity in each cartesian coordinate direction, material density in each cartesian coordinate direction, and coefficient of heat transfer (Thermal Expansion) in each cartesian coordinate direction.

4. BUCK1.OUT: An output file for the buckling of the simply supported boundary conditions of the laminated composite panel. It gives out the system data with regard to the number of equations solved, matrix elements, half bandwidth, Max. & Min. diagonal stiffness matrix values, number of eigenvalues and mode shapes. It prints out for each mode shape the X, Y, and Z displacements as well as rotations. At the end of this output file it lists the time consumed in performing each solution operation.

5. BUCK2.OUT: An output file for the buckling of the encastré (fixed-fixed) boundary conditions of the laminated composite panel. It gives out the system data with regard to the number of equations solved, matrix elements, half bandwidth, Max. & Min. diagonal stiffness matrix values, number of eigenvalues, and mode shapes. It prints out for each mode shape

the X, Y, and Z displacements as well a rotations. At the end of this output file it lists the time consumed in performing each solution operation.

6. T1.SES: An input file for the heat transfer session. It gives in geometry and material properties.

7. T1.MOD: An input file for the heat transfer module. It gives in the material properties, prescribed nodal temperatures from the previous heat transfer analysis together with the degrees of freedoms and the constraints.

8. T1.TEM: An output file giving the temperature results from the heat transfer analysis. It lists the modeling mesh characteristics, solutions time, and it lists the nodal temperatures for each time step.

9. T1.OUT: An output file giving the stress output at each temperature/time step, i.e. thermal stresses output. This file lists both the principle stress (SIGMA) and the shear stress (TAU) in each of the cartesian coordinate directions (X, Y, and Z) for each node. It also lists out the axial and rotational force moments in each of the cartesian coordinate directions (X, Y, & Z). At the end a small solution times log is displayed.

CHAPTER 7

DISCUSSION, CONCLUSIONS, AND SUGGESTIONS FOR FURTHER WORK

This seventh chapter is the discussion, conclusions, and the suggestions for further work. The discussion follows the sequence of the chapters and discusses the analysis explaining and validating the results. The conclusions are summarized in accordance with the flow of the chapters. The suggestions for further work indicate the possibilities of improvements, other applications to be tackled, and experimentation requirements.

DISCUSSION

Laser directed energy weapon systems are relatively a new field. The design, effects, and experience, as well as knowledge of operation, are not widespread. However, such knowledge and expertise can be found in governmental and commercial forms although the literature is not comprehensive.

It was stated at the beginning of this thesis that one of the main objectives was to demonstrate the applicability and flexibility of the finite element method in solving continuum problems in applied military engineering. The present results were compared with those obtained from experimental NRL measurements. The good agreement proves tho applicability of the finite element technique in the present class of problems.

The finite element technique incorporating strain energy method was used to solve the static buckling problem. On the other hand, incorporating the Galerkin weighted residual approach, and primitive variables formulation, is used to solve the variable conductivity general energy equation.

Results of the stress analysis showed accurately the loading distribution, while the temperature results showed clearly and accurately the temperature gradients affecting the thermal stresses leading to buckling and consequent failure. Modeling the pulse buckling response is critical as the structure is directly and instantaneously weakened leading to substantial collapse of the mechanically and thermally loaded panel.

From Figures 6.1, 6.2, and 6.3 it can be seen that the buckling load for the simply supported (S.S.) case showed a half-wave deformation at mode 8 whereas for mode 1 which gives the lowest buckling load two waves appeared for its mode shape. Thus, we consider the buckling mode 1 with lowest critical load as 9.26 pounds per square inch for the S.S. case and 15.9 pounds per square inch as the critical load for the fixed-fixed case in the first mode of buckling.

The simply supported case emulates a wing or a tail of a helicopter while the fixed-fixed case models a part of the main body. Since each time step in the analysis is one (1) second corresponding to temperature steps then buckling critical stress is reached in time step 10 i.e. ten seconds with our 1KW per square centimeter laser load making the panel lowest temperature of 625 F, while at the irradiation section of the panel the maximum temperature is 3750 F.

The stress analysis was performed for temperature distributions that were obtained from the transient heat transfer analysis. This analysis was made for temperatures at time steps 1 and 25. The program allows the reading of temperature quantities at different time steps and use them for thermal stress analysis. The stress units are in pounds per square inch and the Von-Mises stress corresponds to an average equivalent stress used principally for design purposes and calculated in terms of other components.

The negative stress means compressive stress and the positive (+Ve) stress means tensile stress. The thermal stress analysis was performed for the S.S. model for temperature conditions at time steps 1 and 25, since we are considering firing at helicopter tails. However, the required exposure time of 10 seconds is relatively long for weapon system active tracking while firing at a moving target in the same time. The simplest solution is to increase the power of the laser beam from 1KW per square centimeter to 5KW per square centimeter which will result in a panel buckling time of no more than one

second which correspond to the failure times graph found in Dr. Gularte's article, "Failure of Mechanically Loaded Laminated Composites Subjected to Intense Localized Heating."

The stresses are higher near the boundaries due to restrictions imposed to prevent the panel from expansion, therefore these boundary conditions or restrictions of the degrees of freedom induce higher stress away from the laser beam area.

The total strain energy for the S.S. case was 326.7 pounds per inch.

Laminated composites technology to improve the toughness of laminated composite panels is limited. Such improvements are in general usually accompanied by a sacrifice in other properties such as strength at elevated temperatures.

Over the last ten years or so, much effort was concentrated on understanding the failure mechanisms and predicting the strength of compression loaded laminates. The fracture of composites is usually instantaneous and catastrophic, which makes the identification of critical failure modes hard to accomplish. The problem is further complicated because changes in material properties, or the presence of defects, can lead to completely different failure modes. Hence, an analytical model accurate for one material system may not predict failure for another material system.[42] Development of a unified model which can be applied to various composite

---

[42]Hahn and Williams, Compression Failure Mechanics in Unidirectional Composites, p. 2.

material systems and failure modes was not within grasp. However, the current approach as demonstrated in this thesis, can identify critical failure modes for each material system and can develop a unique model for each failure mode.

Laminated composites performance is known to be reduced due to the substantial amount of complex load-induced damage. The heterogeneity nature of the laminated composites acts not just as a crack initiator, but also as a crack arrester.[43] Hence, it is necessary to have a model which accounts for the average effects of interests. This is continuum damage mechanics, which was applied successfully to isotropic media such as metal and concrete. However, the application onto laminated orthotropic composites has not been widespread, or distinctly successful.

The applications objective of continuum damage mechanics models to laminated composites is useful for engineering design purposes. The alternative would be to attempt to solve a highly anisotropic, multiply connected, non-linear, non-symmetrical boundary value problem.

An important feature that stands out for laminated composites is that their composite tensile modulus is greater than their composite compressive modulus. Precise theories to explain this feature are not available. However, one possible explanation is that the fibers themselves are less stiff in compression than in tension. The strain hardening observed for

[43]Allen, Research on Damage Models for Continuous Fiber Composites, pp. 86-App. 7.

graphite/epoxy composites under tension is attributed to improved alignment of internal structure of the graphite fibers during loading. Conversely, initially imperfect alignment of the fiber structure may grow in amplitude during compression loading.[44]

As mentioned initially, we do not have a satisfactory failure criteria for composite materials at room temperature let alone elevated temperatures.

Composite material failure criteria will have to account for the material being stronger in tension than in compression. The elevated temperatures effects exaggerate this, i.e. the matrix provides lateral resistant for the fibers, and as the matrix is heated it softens. The bottom line is that with current fabrication techniques, irradiated structures are markedly more vulnerable in compression.

The results of this work have been studied carefully in order to understand the compression behavior of the locally heated graphite/epoxy laminated composite panel. The predominant failure mode has been identified as shear crippling, due to the high bending strains in the fiber in the post-buckled state. This leads to longitudinal splitting between fibers at shear zone/s because of the required kinematic compatibility. Shear crippling in laminated composite resembles slip lines in metals.[45] The most important difficulty in predicting failure in laminated composite panels is the absence of

---

[44]Hahn and Williams, Compression Failure Mechanics in Unidirectional Composites, p. 12.

[45]Ibid, pp. 16-17.

proven failure criteria capable of handling the complex loading histories characteristic of these responses.[46] However, the buckling response in this work has been captured reasonably well.

Equal and higher laser loading rates, as that used in this work, in conjunction with the laminated composite panel configuration, will almost always result in catastrophic failure.

CONCLUSIONS:

1. Based on the results obtained, the analysis program of the laser-induced damage calculation, in laminated composites panels, of helicopters, using the finite element method, is capable of predicting the response of a structure under compression loading subjected to laser strike. Considering the mathematical assumptions made, and the continuum failure mechanism approach followed, the numerical values computed should be treated as suitable for the conceptual engineering design phase.

2. The analysis program developed in this thesis met the objectives of the thesis study, i.e. it provided enough information and method for the prediction of helicopters laminated composites panels structural response while encountering a laser strike. The analytical simulations have

[46]Prantil, Response of a Thin Cylindrical Shell Under Lateral Impulse Loads, pp. 57-59.

verified the computational methods for studying the non-linear buckling failure response of compression loaded, localized laser heated, laminated composite panels.

3. Although the finite element simulations used here represent the state of the art capability for studying laminated composite panels response, however, the information that can be obtained to perform an accurate laser lethality loads or doses assessment is limited.

4. It is concluded from the stress plots that at higher temperature (time step 25), although stress distribution appears to have the same pattern (as indicated by the stress chart bars of Figures 4 through 7 in chapter 6), the stress quantities were considerably higher.

5. With current fabrication techniques of laminated composites irradiated structures are markedly more vulnerable in compression than tension.

SUGGESTIONS FOR FURTHER WORKS:

1. Inclusion of spallation effects as a requirement in the program output. Incipient spall layer can be one model.

2. Inclusion of ablation effects as a requirement in the program output. Different variations can be modeled.

3. Extension of the present work to models that account for non-linear mechanical and thermal material properties in each of the three dimensions.

4. Inclusion of damping and investigating its effects.

5. Inclusion of a variety of laser loading and beam characteristics, together with different target geometries, and mechanical and thermal properties, e.g. pulse versus continuous laser.

6. Investigation of the compressive shock wave damage.

7. The magnitude of the buckling collapse has been accurately predicted here. This can serve as a relevant input to any future suggested lethality algorithm. Reduction in buckling threshold can represent a very viable lethal response mechanism to be incorporated in such algorithm.

8. Physically performing accurate detailed experimentation program under laboratory conditions for the complete and variable

measurements of all the involved parameters in the laser-induced damage to mechanically loaded laminated composite panels and structures used in helicopters and aeroplanes.

BIBLIOGRAPHY

Aerospace Composites & Materials. Vol. (2,3), Vol. (3), No. (1). London: The Shephard Press Ltd., 1990.

Alghatam, Mohammed J. "An Investigation into the Use of the Finite Element Method for Certain Continuum Problems." Unpublished MSC Thesis, University of Technology, Loughborough, Leics, England, UK, 1979.

_____. "Solar-Powered Air Conditioning System Investigation Using the Finite Element Method," in Solar & Wind Technology, Vol. 4, No. 3. Oxford: Pergamon Press, 1987.

_____. "Solar Ventilation and Air-Conditioning System Investigation Using the Finite Element Method." Unpublished PhD Thesis, University of Technology, Loughborough, Leics, England, UK, 1985.

_____. "The Forced Vibration of Beams and Frameworks Using the Finite Element Method." Unpublished BSC Thesis, Trent Polytechnic, Nottingham, England, UK, 1976.

Allen, David H. Research on Damage Models for Continuous Fiber Composites. Final Technical Report, Aerospace Engineering Department. College Station: Texas A & M University, Texas, USA (1988).

Armanios, Erian A. Analysis of Interlaminar Fracture in Composites Under Combined Loading. Atlanta: Georgia Institute of Technology, 1988.

Bryan, Sheryl K. "Reanalysis Methods for Structures with Laser-Induced Damage," Unpublished MS Thesis, Air Force Inst. of Tech., Wright-Patterson AFB, Ohio, 1983.

Cheung, Y. K. and Yeo, M. F. Practical Introduction to Finite Element Analysis. London: Pitman Publishing Co., 1979.

Clough, Robert W. "The Finite Element Method in Structural Mechanics," in Stress Analysis: Recent Developments in Numerical and Experimental Methods, edited by O. C. Zienkiewicz and G. S. Holister. London: Wiley and Sons Ltd., 1954.

Datta, S. K.; Shah A. H.; Al-Nasser Y.; and Bratton R. Elastic Wave Dispersion in Laminated Composite Plate. Contract N00014-86-K-0280. Bolder: University of Colorado, 1987.

Giuliani, John L. and Mulbrandon, Margaret Numerical Simulation of the Laser-Target Interaction and Blast Wave Formation in the DNA/NRL Laser Experiment. Memorandum Report 5762, U.S. Department of the Navy. Washington, D.C.: Geophysical and Plasma Dynamics Branch, Plasma Physics Division, Naval Research Laboratory, 1986.

Gularte, Ronald C., Head, Engineering Materials Group, Naval Research Laboratory, and Holderby, G., Wright Research and Development Center, Washington, D.C. Privite communications, 1990-1991.

Gularte, Ronald C.; Nemes, J. A.; Stonesifer, F. R.; and Chang, C. I. "Failure of Mechanically Loaded Laminated Composites Subjected to Intense Localized Heating," in International Journal for Numerical Methods in Engineering, Vol. 25. London: Wiley & Sons Ltd., 1988.

Hahn, H.Thomas and Williams, Jerry G. Compression Failure Mechanics in Unidirectional Composites. NASA Technical Memorandum 85834. Langley, VA: NASA, 1984.

Hinton, E. and Owen, D. R. Finite Element Programming. Swansea: Academic Press, 1977.

Huebner, K. H. The Finite Element Method for Engineers. London: Wiley and Sons Ltd., 1975.

Oden, J. Timothy Finite Elements of Non-linear Continua. New York: McGraw-Hill, 1972.

Patankar, S. V. Numerical Heat Transfer and Fluid Flow. New York: Hemisphere Publishing Corporation, McGraw-Hill Book Company, 1980.

Prantil, V. C. Response of a Thin Cylindrical Shell Under Lateral Impulse Loads. Livermore: Structural Mechanics Division, Sandia National Laboratories, 1988.

Reddy, J. N. and Liu, C. F. A Higher-Order Theory for Geometrically Nonlinear Analysis of Composite Laminate. NASA Contract Report 4056. Blacksburg, VA: Virginia Polytechnic Institute and State University, 1987.

Roark, R. J. and Young, W. C. Formulas for Stress and Strain," 5th Ed. New York: McGraw-Hill, 1976.

Scheid, S. "Numerical Analysis," Schaum's Outline Series. New York: McGraw-Hill, 1968.

Segerlind, L. J. Applied Finite Element Analysis. London: Wiley and Sons Ltd., 1976.

Stuart, Mark J. and Hagman, Jane A. Buckling and Failure Characteristics of Graphite-Polyimide Shear Panels. NASA Technical Memorandum 2153. Langley, VA: NASA 1983.

Sun, C. T.; Chen J. K.; and Chang, C. I. "Failure of a Graphite/Epoxy Laminate Subjected to Combined Thermal and Mechanical Loading," J. Compos. Mater., Vol. 19, 1985.

Tang, P. Y. Development of a Progressive Failure Model for Strength of Laminated Composite Structure. San Diego: Naval Ocean Systems Center, 1989.

Timoshenko, S. P. and Gere, J. M. Theory of Elastic Stability," 2nd Ed. New York: McGraw-Hill, 1961.

Underwood, J. H. Applications and Limitations of Finite Element Analysis to Armament Components. Technical Report ARCCB-TR-89018. Watervliet, NY: U.S. Army Armament Research, Development and Engineering Center, Close Combat Armament Center, Benét Laboratories, 1989.

Zienkiewicz, O. C. The Finite Element Method. London: McGraw-Hill Book Company, 1977.

_____. "The Finite Element Method: From Intuition to Generality." Applied Mechanics Review, 19, 1969.

INITIAL DISTRIBUTION LIST

1. Combined Arms Research Library
   U.S. Army Command and General Staff College
   Fort Leavenworth, Kansas 66027-6900

2. Defense Technical Information Center
   Cameron Station
   Alexandria, Virginia 22314

3. Mr. James F. Fox
   Scientific Advisor
   U.S. Army Combined Arms Command
   Fort Leavenworth, Kansas 66027

4. Mr. David I. Drummond
   Department of Sustainment and Resourcing Operations
   U.S. Army Command and General Staff College
   Fort Leavenworth, Kansas 66027

5. CPT George J. Fukumoto
   U.S. Army Combined Arms Command, Combat Development
   Fort Leavenworth, Kansas 66027

6. Dr. Ronald C. Gularte
   Engineering Materials Group
   Naval Research Laboratory
   Washington, District of Columbia 20375-5000

7. Dr.Mehran Lashkari
   Structural Research and Analysis Corporation
   1661 Lincoln Boulevard, Suite 200
   Santa Monica, California 90404

8. Chief of Staff
   Bahrain Defense Force (G.H.Q.)
   Post Office Box 245, Bahrain

9. MAJ Fred Chiaventone
   Department of Joint and Combined Operations
   U.S. Army Command and General Staff College
   Fort Leavenworth, Kansas 66027

10. MAJ Terry Siems
Combat Studies Institute
U.S. Army Command and General Staff College
Fort Leavenworth, Kansas 66027

11. MAJ Anthony J. Cerri
Center for Army Tactics
U.S. Army Command and General Staff College
Fort Leavenworth, Kansas 66027

12. MAJ Eric R. Wildemann
Center for Army Leadership
U.S. Army Command and General Staff College
Fort Leavenworth, Kansas 66027

DEPARTMENT OF THE ARMY
U.S. ARMY COMMAND AND GENERAL STAFF COLLEGE
1 REYNOLDS AVENUE, BUILDING 111
FORT LEAVENWORTH, KANSAS 66027-1352

REPLY TO
ATTENTION OF

ATZL-SWY

2 May 2001

MEMORANDUM FOR ATTN: Larry Downing, DTIC-OCQ, Defense Technical Information Center, 8725 John J. Kingman Road, Suite 0944, Fort Belvoir, VA 22060-6218

SUBJECT: Request for Distribution Change

1. The following documents should be changed from distribution B to distribution A. The limitations have been removed and they are now publicly available.

THESIS	ACCESSION NO
Arracourt—September 1944	ADB067783
Criminal Investigative Activities, World War II and Vietnam, Battlefield Implications	ADB125460
Does the US Army Need a Full-Time Operations Other Than War Unit?	ADB225714
F-16 Low Altitude Navigation and Targeting Infrared System for Night and the Night Close Air S	ADB135971
Finite Element Analysis of Laser-Induced Damage to Mechanically Loaded Laminated Compo	ADB157706
Role of Army Intelligence in the Domestic Drug War	ADB149106
Should Members of the Military be Concerned about Television Coverage of Wartime Operation	ADB135563
Teaching Mission Orders in Officer Advance Course Instruction: Reality or Myth?	ADB135628
The Cut of the Scythe	ADB125547
The Light Infantry Division, Regionally Focused for Low Intensity Conflict	ADB150050
The Role of the Corps Air Defense Artillery Brigade	ADB148423
The Strategic Rationale for Special Operations Forces Employment	ADB157746

2. Thanks. Please let me know when they are done. My e-mail address is burgesse@leavenworth.army.mil, and my phone number is (913) 758-3171.

EDWIN B. BURGESS
Chief, Public Services
Combined Arms Research Library